

~~CONFIDENTIAL~~

SECURITY INFORMATION

RM A52B05

APR 17 1952

UNCLASSIFIED
INP

RESEARCH MEMORANDUM

FULL-SCALE WIND-TUNNEL INVESTIGATION OF THE EFFECTS OF WING
MODIFICATIONS AND HORIZONTAL-TAIL LOCATION ON THE
LOW-SPEED STATIC LONGITUDINAL CHARACTERISTICS
OF A 35° SWEEP-WING AIRPLANE

By Ralph L. Maki

Ames Aeronautical Laboratory
Moffett Field, Calif.

~~CLASSIFICATION CHANGED~~

To Confidential

CLASSIFIED DOCUMENT

This material contains information affecting the National Defense of the United States within the meaning of the espionage laws, Title 18, U.S.C., Secs. 793 and 794, the transmission or revelation of which in any manner to an unauthorized person is prohibited by law.

NATIONAL ADVISORY COMMITTEE
FOR AERONAUTICS

WASHINGTON
April 3, 1952

NACA LIBRARY
LANGLEY AERONAUTICAL LABORATORY
Langley Field, Va.

~~CONFIDENTIAL~~
~~RESTRICTED~~
SECURITY INFORMATION

UNCLASSIFIED

NACA RM A52B05

CLASSIFICATION : CANCELLED

Author: NACA R7 2715 Date 6/12/54

By Maki 11/9/54 See

12/1/53

see NACA R7 7611 on R7 72/10/53



UNCLASSIFIED

NATIONAL ADVISORY COMMITTEE FOR AERONAUTICS

RESEARCH MEMORANDUM

FULL-SCALE WIND-TUNNEL INVESTIGATION OF THE EFFECTS OF WING
MODIFICATIONS AND HORIZONTAL-TAIL LOCATION ON THE
LOW-SPEED STATIC LONGITUDINAL CHARACTERISTICS
OF A 35° SWEEP-WING AIRPLANE

By Ralph L. Maki

SUMMARY

Tests have been made in the Ames 40- by 80-foot wind tunnel to evaluate the effects of wing modifications on the static longitudinal characteristics of a 35° swept-wing airplane. The wing modifications were designed to replace existing wing slats as low-speed high-lift devices. The principal modification incorporated camber over the forward portion of the chord and an increased leading-edge radius. The airplane was tested with the horizontal tail on and off and in a lowered position. All configurations were tested at a Reynolds number of 8.4×10^6 , and some were tested over a range of Reynolds numbers from 3.2×10^6 to 12.3×10^6 .

The full-span modified wing leading edge provided an increment of wing maximum lift somewhat greater than given by the slats. In contrast to the flat-topped lift curves with the slats open, the lift curves of the airplane with the modified wing leading edge were characterized by an abrupt loss of lift beyond maximum lift; further, the airplane with the modified wing leading edge was longitudinally unstable beyond maximum lift, whereas the slats-open configurations were stable. The significance of these changes in characteristics in terms of the flying qualities of the airplane at maximum lift was difficult to judge in view of past inconsistencies between pilot opinions and conclusions drawn from static wind-tunnel-test results.

Additional wing modifications were tested in an effort to alter the characteristics of the airplane with the modified wing so as to compare more closely with the characteristics of the slats-open configuration. One modification was successful both in rounding the lift-curve peak and

~~RESTRICTED~~

UNCLASSIFIED

in providing longitudinal stability beyond maximum lift, but at the expense of a loss in wing maximum lift. This configuration consisted of an outboard 76-percent-span modified leading edge, and a spoiler at the leading edge of the unmodified inboard sections, with a sharp discontinuity between the two portions of the wing leading edge.

The lower horizontal-tail position improved the longitudinal stability of all configurations near maximum lift. With the tail in the lower position, the airplane with the modified wing leading edge had pitching-moment characteristics which were considered acceptable.

INTRODUCTION

Flow separation and its attendant effects on aerodynamic characteristics appear at progressively lower wing lifts as the sweep of wings is increased. Various wing high-lift devices are being used to delay the separation and thus extend the maximum usable lift range of swept wings. Such devices as wing leading-edge slats and leading-edge flaps, in addition to trailing-edge flaps, have proved successful. However, such devices entail complex mechanical installations and add considerable weight to the airplane. Recent studies, such as those of references 1 to 3, have shown that modified wing sections, utilizing moderate amounts of camber over the forward portion of the chord and increased leading-edge radii, also can be designed to delay the occurrence of flow separation to higher lifts. Such high-lift wing sections would eliminate the structural disadvantages of leading-edge devices such as slats.

The primary purpose of the study reported herein was to evaluate the effects on the low-speed static longitudinal characteristics of an F-86A airplane when the existing slats were replaced with a wing-section modification similar to those considered in references 1 to 3. To aid in the design of the modification, the two-dimensional characteristics of the wing sections with slat closed and open were compared with the characteristics of the section with the selected leading-edge modification.

Other studies, such as that of reference 4, have shown that a lowered horizontal-tail position has a favorable effect on the longitudinal stability of swept-wing configurations at high lifts. Accordingly, tests were made on the subject airplane with both the normal and the modified wing leading edges with the horizontal tail at a lowered position.

NOTATION

- A aspect ratio
b wing span
c local chord, measured perpendicular to the wing quarter-chord line
c' local chord, measured parallel to the plane of symmetry

\bar{c} mean aerodynamic chord
$$\left(\frac{\int_0^{b/2} c'^2 dy}{\int_0^{b/2} c' dy} \right)$$

- c_c section chord-force coefficient
 C_D drag coefficient
 C_{DT} drag coefficient due to wind-tunnel-wall interference
 C_L lift coefficient
 c_l section lift coefficient
 C_m pitching-moment coefficient, referred to $0.25\bar{c}$
(See fig. 1.)
 C_{mT} pitching-moment coefficient due to wind-tunnel-wall interference
 c_n section normal-force coefficient
R Reynolds number $\left(\frac{V\bar{c}}{\nu} \right)$
V free-stream velocity
x distance along airfoil chord, referenced to the leading edge of the unmodified airfoil sections
y spanwise distance, measured from the fuselage center line

- z height above the wing reference plane, which is defined by the wing quarter-chord line and the chord of the unmodified section at 0.663η
- α airplane angle of attack, measured with respect to the wing reference plane
- α_0 angle of attack of the two-dimensional models
- α_T increment of airplane angle of attack due to wind-tunnel-wall interference
- δ_f trailing-edge flap deflection, measured perpendicular to the flap hinge line
- η fraction of semispan $\left(\frac{2y}{b}\right)$
- ν kinematic viscosity

Subscripts

- t horizontal tail
- l lower
- u upper
- max maximum

MODELS AND APPARATUS

Two-Dimensional Models

Two-dimensional tests were made of three airfoil sections. The profiles of the three models were: (1) that of the airplane wing section normal to the wing quarter-chord line at 0.857 semispan; (2) the same section with the slat open; and (3) the same section modified by adding camber to the forward portion of the chord and increasing the leading-edge radius. The coordinates of these profiles are given in table I. The models, made of laminated mahogany, had 2-foot chords and spanned the 2-foot height of the 2- by 5-foot open-circuit wind tunnel in which they were tested. Each model was equipped with about 40 pressure orifices at the midspan station.

Full-Scale Airplane

Unmodified airplane.- The investigation of the test airplane was made in the Ames 40- by 80-foot wind tunnel. A three-view sketch of the airplane is shown in figure 1; pertinent geometric data are listed in table II.

The photographs of figure 2 show the airplane mounted on a three-strut support in the wind tunnel. The main landing gear was removed to accommodate fittings for supporting the airplane on the front struts. Loads were transmitted to the rear strut through a boom placed in the fuselage and attached to the horizontal-tail supports and to the aft-fuselage-section attachment lugs. To accommodate the tail-support system, the engine was removed.

The removal of the engine required that the air-intake duct and the cooling ducts on the fuselage be sealed for all the tests. For most of the tests these were the only seals added to the airplane. For certain tests, however, the gaps between the slat segments (see fig. 1) were sealed and, with the slats closed, the slat-to-wing junctures also were sealed.

Coordinates of the wing sections normal to the wing quarter-chord line at 0.467 and 0.857 semispan are given in table III; these coordinates are given with respect to the wing reference plane which is defined by the panel quarter-chord line and the chord of the section at 0.663 semispan taken normal to the wing quarter-chord line. Profiles of a typical wing section with slat closed and open are given in figure 3(a).

Modifications.- A full-span application was made of the modified wing section tested two-dimensionally. A typical profile of the modified section is shown in figure 3(b). The full-scale modification was effected by replacing the leading edges of the wing with wood blocks contoured to the modified-section coordinates. The installation, referred to as wing modification 1, is shown in the photograph of figure 4. Coordinates of the modified sections normal to the wing quarter-chord line at 0.467 and 0.857 semispan are given in table IV.

The modified wing sections were later cut back to the original sections from the wing-fuselage juncture to 0.242 semispan. With a smooth fairing used between the two portions of the wing, the configuration is referred to as wing modification 2. With a sharp discontinuity used between the two portions and with a spoiler extending from the fuselage to 0.242 semispan, the configuration is referred to as wing modification 3. These modifications are shown in figures 5, 6, and 7.

The alternate horizontal-tail position used for some of the tests, described in figure 1, lowered the horizontal tail from 0.208 η to 0.103 η above \bar{c} . The installation is shown in the photograph of figure 8.

TESTS AND RESULTS

Two-Dimensional Tests

The two-dimensional models were tested at a Reynolds number of 2.1×10^6 over an angle-of-attack range from -6° to well beyond maximum lift. The tests consisted of pressure-distribution measurements which were integrated over the chord to determine the section normal-force coefficients. Section lift coefficients were determined for only a few test points according to the expression

$$c_l = c_n \cos \alpha_0 - c_c \sin \alpha_0$$

since it was found that there were only negligible differences between the normal-force and lift coefficients. The test results are presented in figure 9.

Full-Scale Tests

The three-dimensional test results are presented in figures 10 to 18; table V serves as a guide to facilitate reference to the figures. Three-component force characteristics were measured on all configurations at a dynamic pressure of approximately 35 pounds per square foot. This corresponds to a Reynolds number of about 8.4×10^6 based on the mean aerodynamic chord, and approximates the Reynolds number at which flight tests indicate the onset of stall on the airplane in the landing approach. Tuft photographs were taken at selected angles of attack for several configurations at this same Reynolds number. Force data recorded while the tufts were on the wing indicated no significant changes in aerodynamic characteristics due to their presence. Several configurations were tested over a range of Reynolds numbers from 3.2×10^6 to 12.3×10^6 ; the Mach number varied from 0.06 to 0.23 for this range. All configurations were tested over an angle-of-attack range from 0° to beyond stall.

All the tests were made with the trailing-edge flaps deflected either 0° or 38° (maximum deflection). The ailerons and rudder were set in the undeflected positions. For tests with the horizontal tail on, the elevator and horizontal stabilizer were set at 0° with respect

to the wing reference plane. The wing slats were locked in either the closed or the open position, and were unsealed except for the test results presented in figure 11.

CORRECTIONS

No corrections were applied to the two-dimensional data.

The three-dimensional data have been corrected for stream-angle inclination, wind-tunnel-wall interference, and the interference effects of the support struts. The corrections used were those for an unswept, untapered wing. The wall-interference corrections added were as follows:

$$\alpha_T = 0.60 C_L$$

$$C_{DT} = 0.011 C_L^2$$

$$C_{mT} = 0.008 C_L \text{ (tail-on data only)}$$

The effects of sealing the fuselage intake duct and the interference effects of the landing-gear stub struts used to mount the airplane on the lift struts are unknown.

DISCUSSION

Design of Wing Modification 1

The design of the proposed type of leading-edge modification was approached from two-dimensional maximum lift considerations. This approach was selected on the basis of the analysis presented in reference 3, which showed that initial stall on a swept wing is directly related to the stalling characteristics of the airfoil section taken normal to the wing quarter-chord line at the spanwise location of initial stall. In the case of the F-86A airplane, flight tests indicated that initial stall occurred near 0.86 semispan. Consequently, the section normal to the wing quarter-chord line at this span station was used to evaluate the section maximum lift with the slat extended and thus establish a criterion for the selection of a leading-edge modification. The results of the two-dimensional tests (fig. 9) showed that the slat increased $c_{l_{max}}$ of the unmodified section by 0.71.

Theoretical pressure distributions were computed for the section with several arbitrary leading-edge modifications. The distributions were adjusted to such c_l values that the pressure coefficients at 0.005c were all equal to the pressure measured at this chord station on the unmodified section at $c_{l_{max}}$. These c_l values were used as the approximate $c_{l_{max}}$ provided by the various modifications. These studies indicated that more than 2-percent camber in addition to a 2-percent-chord leading-edge radius probably would be needed to equal the $c_{l_{max}}$ of the unmodified section with the slat extended. However, it was felt that the magnitude of the modification should be held to a minimum because of possible adverse effects of large section changes on the high-speed aerodynamic characteristics. In view of these considerations, the modification described in table I was selected for testing. The two-dimensional test results (fig. 9) showed that the selected leading-edge modification increased $c_{l_{max}}$ by only 0.46 or 0.25 less than provided by the slat. Additional section modifications to obtain an increment of $c_{l_{max}}$ equal to that of the slat were not tried since, as indicated above, any further increase in camber was considered undesirable from a high-speed standpoint.

The leading-edge modification was applied over the full span of the wing rather than over the partial span used for the slats, since an analysis by the method of reference 3 indicated that the highest lift effectiveness would result thereby.

Test Results for the Airplane

The high-lift effectiveness of the slats and wing modifications will be examined on the basis of the value of maximum lift,¹ the longitudinal stability at maximum lift, and the shape of the lift curve near maximum lift. The character of the lift-curve peak is examined on the presumption that well-rounded peaks are indicative of (1) adequate stall warning to the pilot, probably noticeable in the form of buffeting, and (2) less severe rolling tendencies at the stall; both by virtue of a more gradual stall progression on the wing. It should be noted that longitudinal stability at stall and a rounded lift-curve peak cannot be considered as absolute criteria since the evidence of flight-test results is not always in accord with conclusions drawn from these criteria.

¹It will be noted in the test results that, because of the moderate sweepback of the wing, the wing lift at which significant changes occur in the aerodynamic characteristics is nearly equal to the wing maximum lift. Hence, reference will be made to $C_{L_{max}}$ as representing the occurrence of initial stall on the wing.

The most pertinent data are those obtained at the Reynolds number of 8.4×10^6 , corresponding to the landing-approach condition. The results at other Reynolds numbers will be briefly considered.

Unmodified wing with slats.- The slats increased $C_{L_{max}}$ from 1.09 to 1.34 with flaps up and from 1.33 to 1.64 with flaps down (fig. 10(a)). The airplane was longitudinally stable beyond maximum lift only when the slats were extended. The lift curves of the four configurations are all quite flat in the region of maximum lift. With slats open and flaps up, the lift remains within about 0.05 of $C_{L_{max}}$ over an angle-of-attack range of 20° to 29° (the maximum tested).

A comparison of the results presented in figures 10(a) and 10(b) shows that the horizontal tail in the normal position did not materially alter the longitudinal stability beyond stall.

The results presented in figure 11 show that the lift effectiveness of the wing was influenced by leakage around the slats. With the slats in the retracted position and with all gaps sealed, $C_{L_{max}}$ was increased by an increment of 0.10, and the drag was reduced throughout the lift range. With the slats extended and with the gaps between the slat segments sealed C_L was still increasing at the highest angle of attack tested; at this angle of attack it exceeded $C_{L_{max}}$ for the unsealed condition by an increment of 0.12.

Wing modification 1.- The $C_{L_{max}}$ of the airplane with the modified wing sections was 1.42 and 1.72 with flaps up and down, respectively, (fig. 12(a)). Thus the increment in maximum lift coefficient provided by wing modification 1 was 0.08 greater than for the slats with flaps both up and down. This was apparently due in part to the greater span of the modification compared to the slats, and in part to the leakage effect noted for the slat configurations.

Although wing modification 1 produced the desired high maximum lift, it was not as satisfactory as the slats with respect to the other two criteria mentioned previously. First, the airplane with wing modification 1 was longitudinally unstable, both with flaps up and flaps down, beyond maximum lift. Second, in contrast to the flat-topped lift curves with slats extended, the lift decreased abruptly beyond maximum lift with wing modification 1.

A comparison of the results presented in figures 12(a) and 12(b) shows that the horizontal tail in the normal position did not significantly affect the longitudinal stability beyond maximum lift.

Reynolds number effects.- The effects of changes in Reynolds number on the characteristics of several of the configurations thus far discussed

are presented in figures 13 and 14. The variation of $C_{l_{max}}$ with Reynolds number, summarized in figure 15, shows that the results at all higher Reynolds numbers were similar to the results at 8.4×10^6 . With decreasing Reynolds number, however, $C_{l_{max}}$ with wing modification 1 decreases more rapidly than with the slats extended.

The character of the lift curves near maximum lift was not significantly altered with variations in Reynolds number.

The longitudinal-stability characteristics beyond maximum lift for most configurations did not significantly change with changes in Reynolds number. However, with slats open and flaps down, the airplane was unstable at the lowest Reynolds numbers; this instability disappeared with increasing Reynolds number.

Additional wing modifications.- To aid in determining possible measures to alter the abrupt lift-curve peak and unstable pitching-moment characteristics beyond maximum lift of the airplane with wing modification 1, the stalling characteristics of all wing configurations were evaluated by means of tuft studies. The photographs with the slats extended (fig. 16(c)) indicate an area of flow separation near the wing root that was not evident with the slats closed (fig. 16(a)). It was believed that this separation was responsible for the favorable C_m variations at high lifts for the slats-open configurations as observed in the results presented in figures 10(a) and 10(b). In an attempt to produce such an area of stall near the wing root, the other wing modifications described in table VI were investigated. The primary purpose of each item in table VI is indicated by its designation as either a stall-generating or a boundary-layer-control device.

The combination of devices designated as wing modification 3 (fig. 5, detail B) was the only modification which provided the desired longitudinal stability, both flaps up and flaps down (fig. 17). With the flaps up, the lift curve was flat topped, and with flaps down the abruptness of the peak was somewhat alleviated. With the flaps up, wing modification 3 provided a value of $C_{l_{max}}$ which was 0.21 lower than with the slats open, and 0.29 lower than with wing modification 1.

Results obtained with the configuration designated as wing modification 2 also are given since they are typical of the results obtained with most of the other modifications. A slight rounding of the lift-curve peak was obtained with flaps up, but there was no improvement in the longitudinal stability at maximum lift (fig. 17). Visual observations of the flow, as evidenced by tuft action, indicated an area of separation near the wing root localized near the wing leading edge. Apparently the spanwise boundary-layer drainage allowed the separated flow to reattach to the wing surface, thus preventing section stall.

The success of wing modification 3 is attributed to the fact that the spanwise drainage of the boundary layer from the inboard region of the wing did not occur. Tuft studies showed the flow actually to be directed inboard. Hence the spoiler over the inboard part of the span was as effective in producing early section stall as it is in two-dimensional flow. The obstruction of the usual spanwise boundary-layer drainage is believed to have been due to an effect of the sharp discontinuity in the wing leading edge at 0.242 semispan. It was concluded from the tuft studies that a strong vortex was shed at the discontinuity. The rotation of a vortex from the discontinuity would be in the proper direction to direct the boundary-layer flow inboard and thus counteract the normal outboard drainage. Examination of the tufts indicated that the sharp discontinuity in the wing leading edge with the slats extended had a similar effect.

Effects of an alternate horizontal-tail position.- The results of tests of the airplane with the horizontal tail in the lower position (fig. 18) indicated definite longitudinal-stability improvements at high lifts for all configurations. With this alternate horizontal-tail location, the airplane with wing modification 1 had pitching-moment characteristics which were believed to be acceptable.

Comparison of Test Results With Predictions

The procedure of reference 3 has been applied to predict the C_L at which initial stall occurs on the wing for several of the configurations tested. The two-dimensional test results described in this paper were used for the predictions together with estimates of the flap effectiveness made from the data in reference 5. The method of reference 3 also was used to estimate the airplane longitudinal stability beyond stall.

The point of sudden drag rise observed in the force-test results was used to indicate the C_L for initial stall for comparison with the predicted values. A summary of the predicted and measured results is given in table VII. The measured results presented are those for the lowest Reynolds number at which the airplane was tested ($R, 3.2 \times 10^6$), since the effective Reynolds number of the wing sections (sections taken normal to the wing quarter-chord line, and based on the component of free-stream velocity in this direction) then most nearly corresponded to the Reynolds number of the two-dimensional tests (2.1×10^6). The method of reference 3 does not consider the effects of a horizontal tail; hence the comparisons were made with tail-off data when available. The predicted C_L for initial stall was conservative in all cases. The increases in C_L for initial stall provided by the various high-lift

devices were predicted quite well, differing from the measured results by no more than 0.07 in any case where tail-off data was available, and differing by 0.13 for the case with the horizontal tail on. The qualitative estimates of the airplane longitudinal stability beyond stall were satisfactory.

CONCLUDING REMARKS

A full-span modified wing leading edge, which incorporated camber over the forward portion of the chord and had an increased leading-edge radius, provided increments of wing maximum lift coefficient at least 0.08 greater than given by the wing slats, both with flaps up and flaps down, at Reynolds numbers from 8.4×10^6 to 12.3×10^6 . The results at lower Reynolds numbers were less favorable. With the slats extended, the unmodified airplane was longitudinally stable beyond maximum lift and displayed a flat-topped lift curve near maximum lift. However, with the modified wing leading edge, the airplane was longitudinally unstable beyond maximum lift and the lift-curve peaks were quite abrupt.

The airplane with the modified wing leading edge was made longitudinally stable and also, with flaps up, displayed a flat-topped lift curve when low maximum-lift sections were used near the wing root, and a means of obstructing the spanwise boundary-layer drainage over this region (in this case, a sharp leading-edge discontinuity) was provided. These changes were accompanied by a loss in $C_{l_{max}}$ of 0.29 and 0.24 with flaps up and down, respectively, below the results with the full-span modification.

Lowering the horizontal tail had a stabilizing effect on all configurations tested. The airplane with the full-span wing modification had pitching-moment characteristics which were considered acceptable with this alternate horizontal-tail position.

Predictions of the wing lift coefficient for initial stall by the method of reference 3 for several wing configurations were conservative. The increases in C_l for initial stall provided by the various high-lift configurations were predicted quite well. Qualitative estimates of the longitudinal stability beyond maximum lift were satisfactory.

Ames Aeronautical Laboratory
National Advisory Committee for Aeronautics
Moffett Field, Calif.

REFERENCES

1. James, Harry A., and Dew, Joseph K.: Effects of Double-Slotted Flaps and Leading-Edge Modifications on the Low-Speed Characteristics of a Large-Scale 45° Swept-Back Wing With and Without Camber and Twist. NACA RM A51D18, 1951.
2. Demale, Fred A., and Sutton, Fred B.: The Effects of Increasing the Leading-Edge Radius and Adding Forward Camber on the Aerodynamic Characteristics of a Wing With 35° of Sweepback. NACA RM A50K28a, 1951.
3. Maki, Ralph L.: The Use of Two-Dimensional Section Data to Estimate the Low-Speed Wing Lift Coefficient at Which Section Stall First Appears on a Swept Wing. NACA RM A51E15, 1951.
4. Furlong, G. Chester, and Bollech, Thomas V.: Downwash, Sidewash, and Wake Surveys Behind a 42° Sweptback Wing at a Reynolds Number of 6.8×10^6 With and Without a Simulated Ground. NACA RM 18G22, 1948.
5. Cahill, Jones F.: Two-Dimensional Wind-Tunnel Investigation of Four Types of High-Lift Flap on an NACA 65-210 Airfoil Section. NACA TN 1191, 1947.

TABLE I.- COORDINATES OF THE TWO-DIMENSIONAL MODELS
[Dimensions given in percent of chord]

Basic profile			Slat lower surface		Airfoil surface beneath slat		Modified leading edge		
x	z _u	z _l	x	z	x	z	x	z _u	z _l
0	-0.16	- - -	3.84	-2.60	3.89	-2.57	-1.98	-2.15	- - -
.14	.44	-0.74	4.96	-1.08	5.66	-.71	-1.50	-.73	-3.48
.28	.67	-.96	6.05	-.06	7.33	.44	-1.00	-.16	-3.89
.47	.89	-1.17	7.14	.74	8.99	1.31	-.50	.31	-4.14
.70	1.11	-1.40	8.23	1.40	10.66	2.01	0	.72	-4.28
1.17	1.44	-1.73	9.32	1.94	12.32	2.60	.50	1.06	-4.39
2.34	2.02	-2.28	11.50	2.79	15.66	3.57	1.00	1.37	-4.43
4.69	2.75	-2.98	13.68	3.44	18.99	4.35	1.50	1.64	-4.46
7.03	3.25	-3.45	14.77	3.70	20.66	4.67	2.00	1.88	-4.47
9.37	3.64	-3.81					2.50	2.07	-4.46
14.05	4.20	-4.32					3.48	2.43	-4.42
18.75	4.62	-4.68					5.00	2.83	-4.35
23.40	4.93	-4.92					7.50	3.36	-4.30
28.10	5.15	-5.08					10.00	3.73	-4.30
32.80	5.29	-5.16					12.50	4.05	-4.37
37.50	5.37	-5.17					15.00	4.29	-4.45
42.10	5.35	-5.10					17.50	4.51	-4.58
46.80	5.27	-4.96					18.70	4.58	-4.67
51.50	5.11	-4.75					23.40	4.93	-4.92
56.20	4.88	-4.45					L.E.radius: 2.00, center at (0.02, -2.15)		
60.90	4.58	-4.08							
65.60	4.20	-3.65					<div> <div>Slat position when extended</div> <div>Deflection, degrees (leading edge down) . . 10</div> <div>Leading-edge position:</div> <div> <div>x -12.34</div> <div>z -2.06</div> </div> </div>		
70.30	3.77	-3.15							
^a 75.00	3.26	-2.58							
100.00	.51	.51							
L.E.radius: 1.303, center at (1.303, -0.15)									

^aStraight lines from
75-percent chord to
trailing edge.

NACA

TABLE II.- GEOMETRIC DATA ON THE F-86A TEST AIRPLANE

Wing	
Area, square feet	287.90
Span, feet	37.12
Aspect ratio	4.79
Taper ratio51
Dihedral angle, degrees	3
Mean aerodynamic chord, feet	8.09
Sweepback of the quarter-chord line, degrees	35.2
Incidence of the root chord, degrees	1
Incidence of the tip chord, degrees	-1
Twist, degrees (washout)	2
Trailing-edge flap (data for one side only)	
Area, square feet	16.26
Span of one flap, feet	6.70
Chord, constant, feet	2.47
Maximum deflection, degrees	38
Gap, percent of wing chord	1.5
Overhang, percent of wing chord	2.0
Inboard end of flap, feet from airplane center line	2.48
Leading-edge slat (data for one side only)	
Area, projected into wing-chord plane, square feet	17.72
Span, feet	12.94
Chord, constant, feet	1.37
Ratio of slat span to wing semispan70
Inboard end of slat, feet from airplane center line	4.50
Deflection when extended, degrees	10
Horizontal tail	
Total area, square feet	35.28
Span, feet	12.75
Aspect ratio	4.65
Taper ratio45
Dihedral angle, degrees	10
Mean aerodynamic chord, feet	2.89
Sweepback of the quarter-chord line, degrees	34.6
Fuselage	
Over-all length, feet	34.20
Maximum width, feet	5.00
Fineness ratio	6.8

TABLE III.- COORDINATES OF THE WING AIRFOIL SECTIONS NORMAL
TO THE WING QUARTER-CHORD LINE AT TWO SPAN STATIONS
[Dimensions given in inches]

Section at 0.467 semispan			Section at 0.857 semispan		
x	z		x	z	
	Upper	Lower		Upper	Lower
0	0.231	- - -	0	-0.098	- - -
.119	.738	-0.307	.089	.278	-0.464
.239	.943	-.516	.177	.420	-.605
.398	1.127	-.698	.295	.562	-.739
.597	1.320	-.895	.443	.701	-.879
.996	1.607	-1.196	.738	.908	-1.089
1.992	2.104	-1.703	1.476	1.273	-1.437
3.984	2.715	-2.358	2.952	1.730	-1.878
5.976	3.121	-2.811	4.428	2.046	-2.176
7.968	3.428	-3.161	5.903	2.290	-2.401
11.952	3.863	-3.687	8.855	2.648	-2.722
15.936	4.157	-4.064	11.806	2.911	-2.944
19.920	4.357	-4.364	14.758	3.104	-3.102
23.904	4.480	-4.573	17.710	3.244	-3.200
27.888	4.533	-4.719	20.661	3.333	-3.250
31.872	4.525	-4.800	23.613	3.380	-3.256
35.856	4.444	-4.812	26.564	3.373	-3.213
39.840	4.299	-4.758	29.516	3.322	-3.126
43.825	4.081	-4.638	32.467	3.219	-2.989
47.809	3.808	-4.452	35.419	3.074	-2.803
51.793	3.470	-4.202	38.370	2.885	-2.574
55.777	3.066	-3.891	41.322	2.650	-2.302
59.761	2.603	-3.521	44.273	2.374	-1.986
^a 63.745	2.079	-3.089	^a 47.225	2.054	-1.625
83.681	-.740	- - -	63.031	.321	- - -
L.E.radius: 1.202, center at (1.201, 0.216)			L.E.radius: 0.822, center at (0.822, -0.093)		

^aStraight lines to trailing edge.

NACA

TABLE IV.- COORDINATES OF THE MODIFIED WING LEADING EDGE AT
TWO SPAN STATIONS, NORMAL TO THE WING QUARTER-CHORD LINE
[Dimensions given in inches]

Section at 0.467 semispan			Section at 0.857 semispan		
x	z		x	z	
	Upper	Lower		Upper	Lower
-1.692	-1.445	- - -	-1.250	-1.359	- - -
-1.273	-.348	-2.552	-.934	-.495	-2.192
-.855	.222	-2.898	-.619	-.099	-2.454
-.436	.629	-3.114	-.304	.197	-2.609
-.018	.969	-3.272	.011	.456	-2.701
.400	1.266	-3.391	.326	.675	-2.769
.819	1.527	-3.473	.641	.867	-2.796
1.237	1.760	-3.523	.956	1.040	-2.813
1.655	1.952	-3.549	1.272	1.189	-2.821
1.992	2.104	- - -	1.476	1.273	- - -
2.074	- - -	-3.552	1.587	- - -	-2.813
2.911	- - -	-3.531	2.217	- - -	-2.787
4.166	- - -	-3.481	3.163	- - -	-2.742
6.258	- - -	-3.472	4.739	- - -	-2.709
8.350	- - -	-3.542	6.314	- - -	-2.712
10.442	- - -	-3.657	7.890	- - -	-2.751
14.626	- - -	-3.956	9.466	- - -	-2.808
15.936	- - -	-4.064	11.042	- - -	-2.885
			11.806	- - -	-2.944
L.E.radius: 1.674, center at (-0.018, -1.445)			L.E.radius: 1.261, center at (0.011, -1.359)		



TABLE V.- SUMMARY OF CONFIGURATIONS TESTED AND DATA PRESENTED

Figure No.	Configuration			Reynolds number	Data	
	Wing	Flaps	Horizontal tail			
10(a)	Slats closed and open	Up and down	Normal	8.4×10^6	C_L vs C_D, α, C_m	
(b)			Off			
11	Slats closed and open, sealed and unsealed	Up	Normal			
12(a)	Modification 1	Up and down				
(b)		Off				
13(a)	Slats closed	Up Down Up Down	Normal	Variable		
(b)	Slats open					
(c)	Modification 1					
(d)						
(e)						
14(a)	Slats closed	Up	Off			$C_{L_{max}}$ vs R
(b)	Slats open	Down				
(c)	Modification 1	Up				
(d)		Down				
15	Slats closed and open, and modification 1	Up and down	Normal			
16(a)	Slats closed	Up	Normal	8.4×10^6	Tuft studies	
(b)		Down				
(c)		Up				
(d)		Down				
(e)	Modification 1	Up				
(f)		down				
17(a)	Slats open, and modifications 1,2, and 3	Up			C_L vs C_D, α, C_m	
(b)	Down					
18	Slats closed and open, and modification 1	Up and down	Low position			

NACA

TABLE VI.- SUMMARY OF ADDITIONAL MODIFICATIONS AND DEVICES
USED WITH WING MODIFICATION 1

NOTATION			
Item	Stall device	Item	Boundary-layer device
1	Wing mod. 2	a	Sharp discontinuity, large gap
2	45° wedge spoiler	b	Sharp discontinuity, small gap
3	60° wedge spoiler	c	Delta vortex generator
4	4-inch-high plug spoiler	d	Fence
5	7-inch-high plug spoiler	e	Vortex generator, small
		f	Vortex generator, large

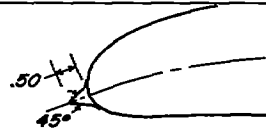
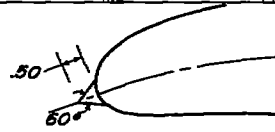

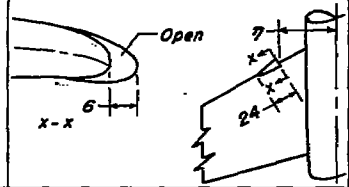
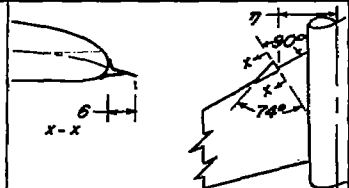
CONFIGURATIONS TESTED						
Item	Sketch (Dimensions in inches except as noted)	δ_f , deg	Spanwise location, η		Chordwise location, x/c	
			Stall device	Boundary-layer device	Stall device	Boundary-layer device
1	See fig. 5, detail A	0.36	.134 - .242			
2		0	.134 - .242		L.E.	
3		0	.134 - .252		L.E.	
		0.36	.134 - .242			
3	As above	0	.134 - .242		.055	
4		0	.134 - .273		.70 at mid-span, mounted normal to ∇	
5	As above, but 7 inches high	0	.134 - .273		As above	
a		0		.242		L.E.
c		0		.242		L.E.

TABLE VI.- CONCLUDED

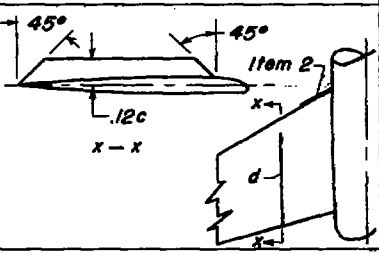
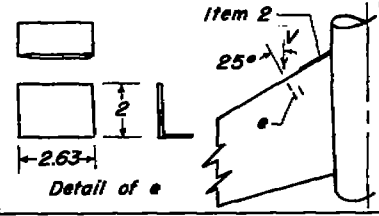
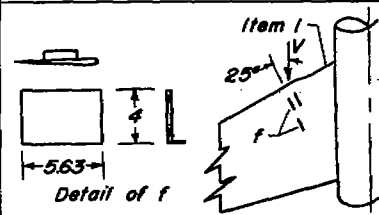
CONFIGURATIONS TESTED						
Item	Sketch (Dimensions in inches except as noted)	δ_r , deg	Spanwise location, η		Chordwise location, x/c	
			Stall device	Boundary - layer device	Stall device	Boundary - layer device
2a		0, 35	.134 - .242	.242	L.E.	L.E.
		0	.134 - .205	.205		
		0	.134 - .252	.252		
2c		0	.134 - .242	.242	L.E.	L.E.
2d		0	.134 - .242	.275	L.E.	.15 to T.E.
2e		0	.134 - .242	.242 and .264	L.E.	.165
5a		0	.134 - .273	.242	.70 at mid-span, mounted normal to V	
1a		0, 35	.134 - .242	.242	L.E.	L.E.
1b		0, 35	.134 - .242	.242	L.E.	L.E.
1f		0	.134 - .242	.272 and .290	L.E.	.18
		0, 35	.134 - .242	.272, .290; .256		.18 .40
		35	.134 - .242	.272 and .290		.06
1,2b	See fig. 5, detail B (wing mod. 3)	0, 35	.134 - .242	.242	L.E.	L.E.

TABLE VII.- COMPARISON OF PREDICTED AND MEASURED LIFT COEFFICIENTS FOR INITIAL STALL
AND LONGITUDINAL STABILITY BEYOND INITIAL STALL; $R, 3.2 \times 10^5$

Wing configuration	Horizontal tail	C_L for initial stall		Increase in C_L for initial stall		Longitudinal stability beyond initial stall	
		Predicted	Measured	Predicted	Measured	Predicted	Measured
Slats closed, flaps up	Off	0.74	0.90	0	0	Unstable	Unstable
Slats open, flaps up	On	.84	1.13	.10	.23	Stable	Stable
Slats open, flaps down	Off	1.40	1.51	.66	.61	Stable	Neutral
Modification 1, flaps up	Off	.99	1.22	.25	.32	Unstable	Unstable
Modification 1, flaps down	Off	1.35	1.47	.61	.57	Unstable	Unstable



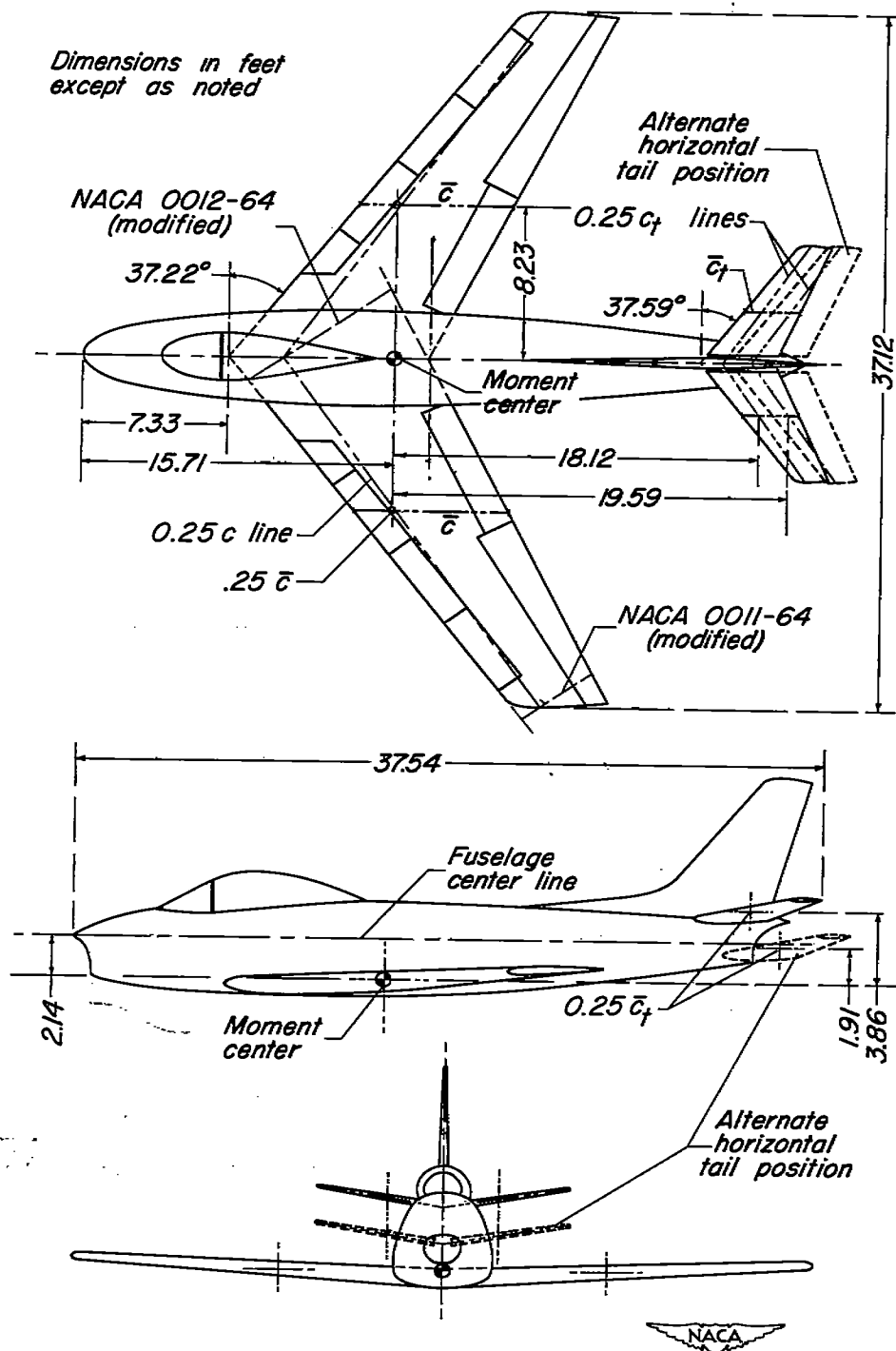
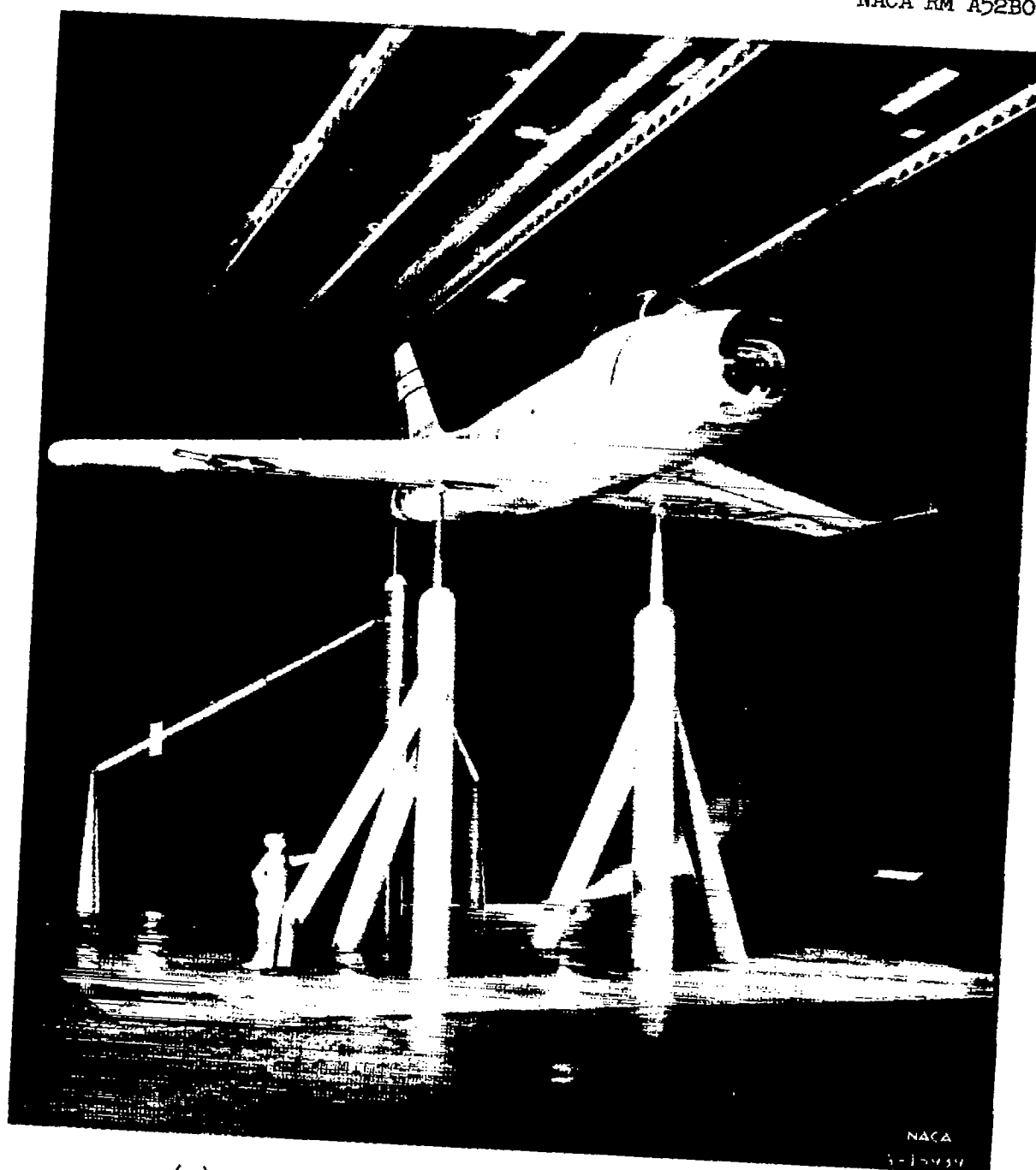
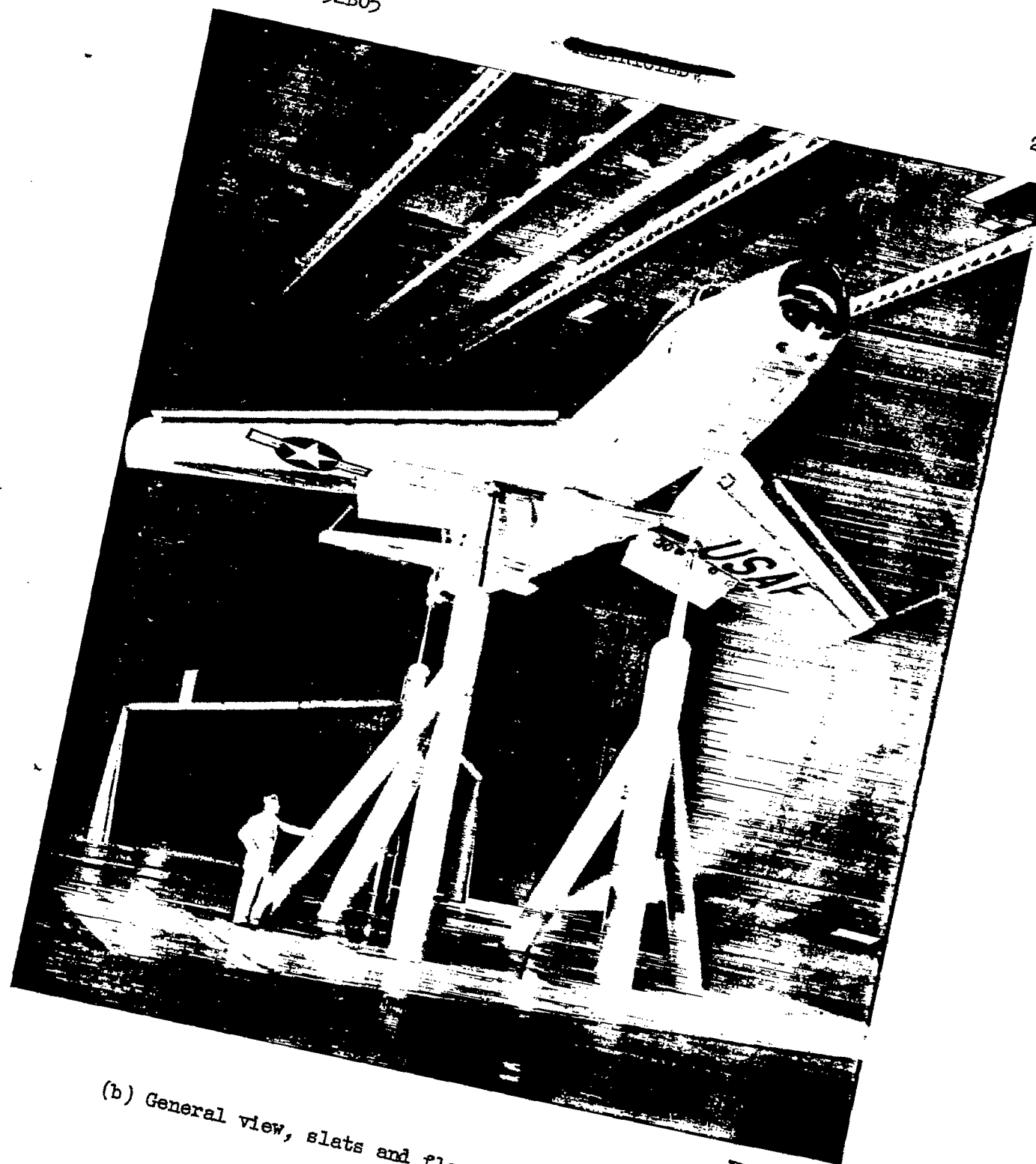


Figure 1.— Three-view sketch of the test airplane.

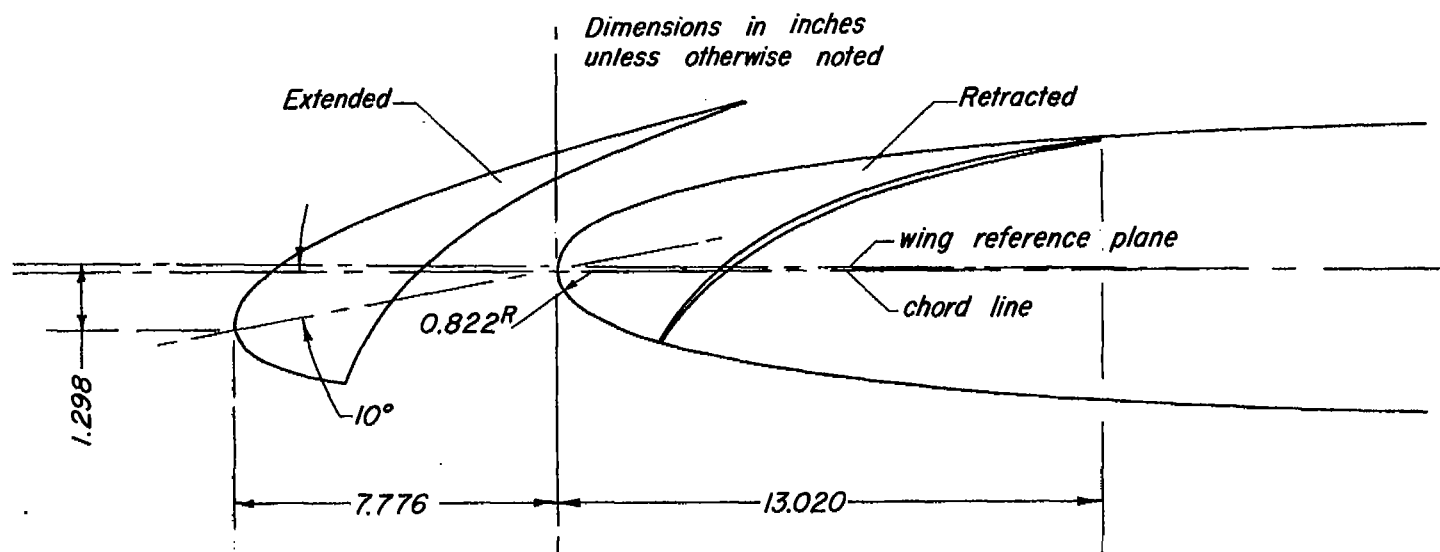


(a) General view, slats and flaps retracted.

Figure 2.- Views of the test airplane mounted in the Ames 40- by 80-Foot wind tunnel.



(b) General view, slats and flaps extended; $\alpha = 16^\circ$
Figure 2.- Concluded.

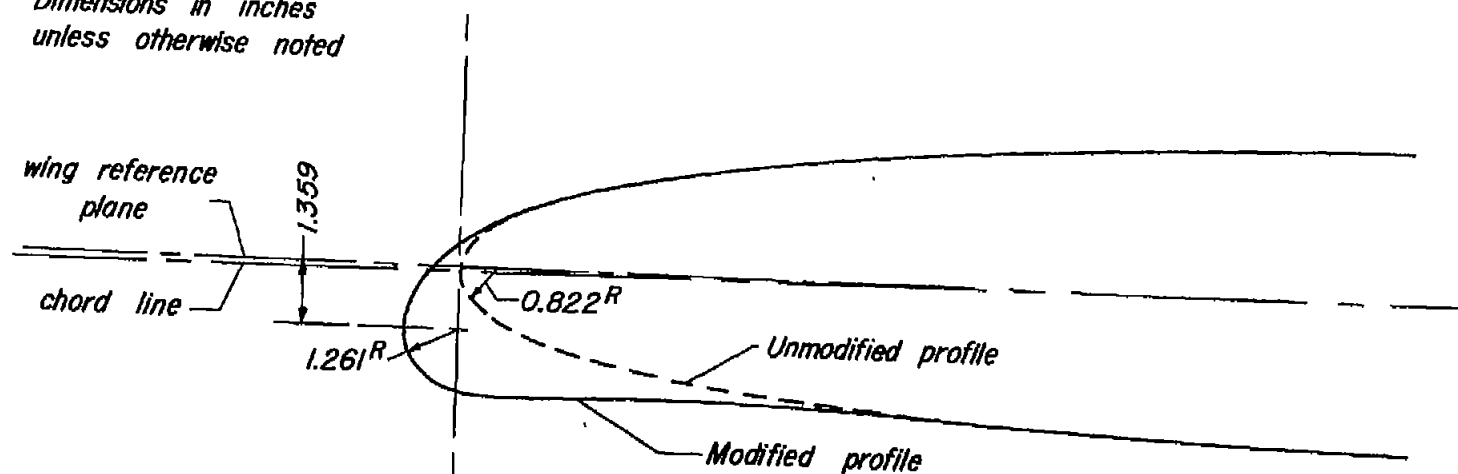


(a) Unmodified section showing slat extended and retracted.



Figure 3.- Details of the wing airfoil sections at 0.857 semispan, taken normal to the wing quarter-chord line.

Dimensions in inches
unless otherwise noted



(b) Modified leading edge.



Figure 3.- Concluded.

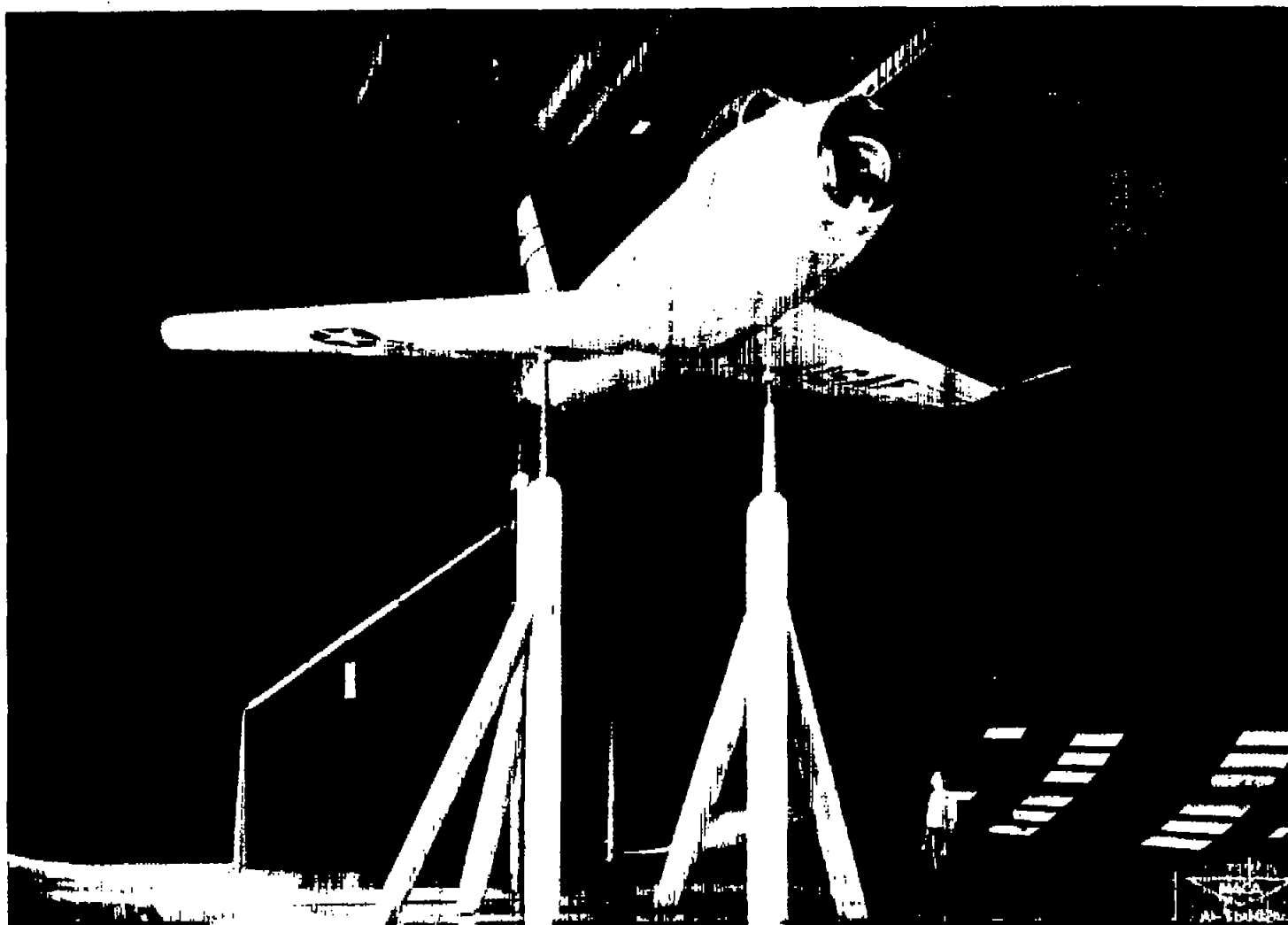
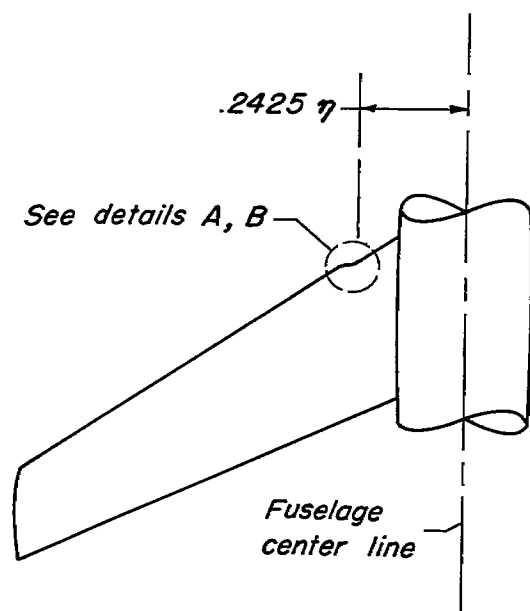
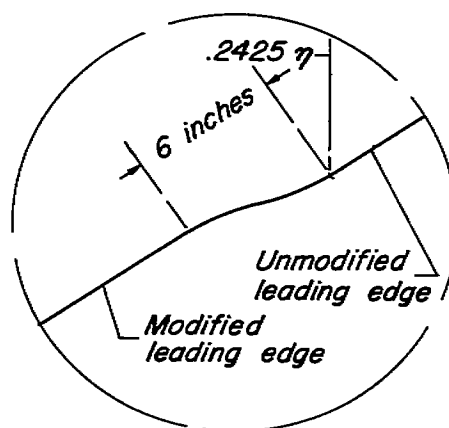


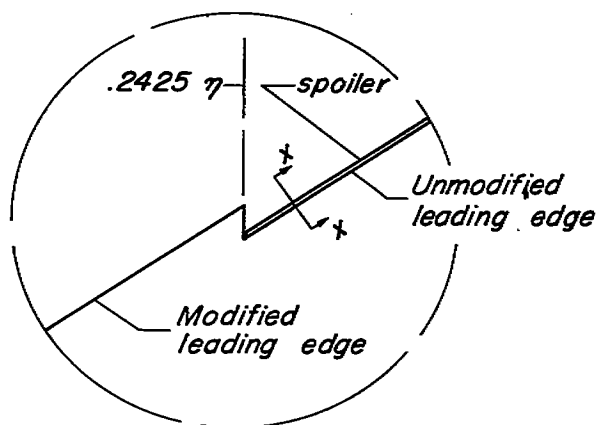
Figure 4.— View of the test airplane with wing modification 1.



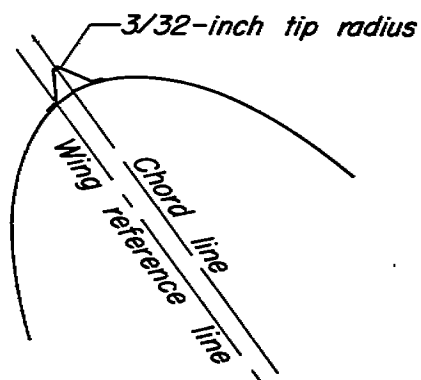
Plan view of left wing



Detail A — Wing mod. 2



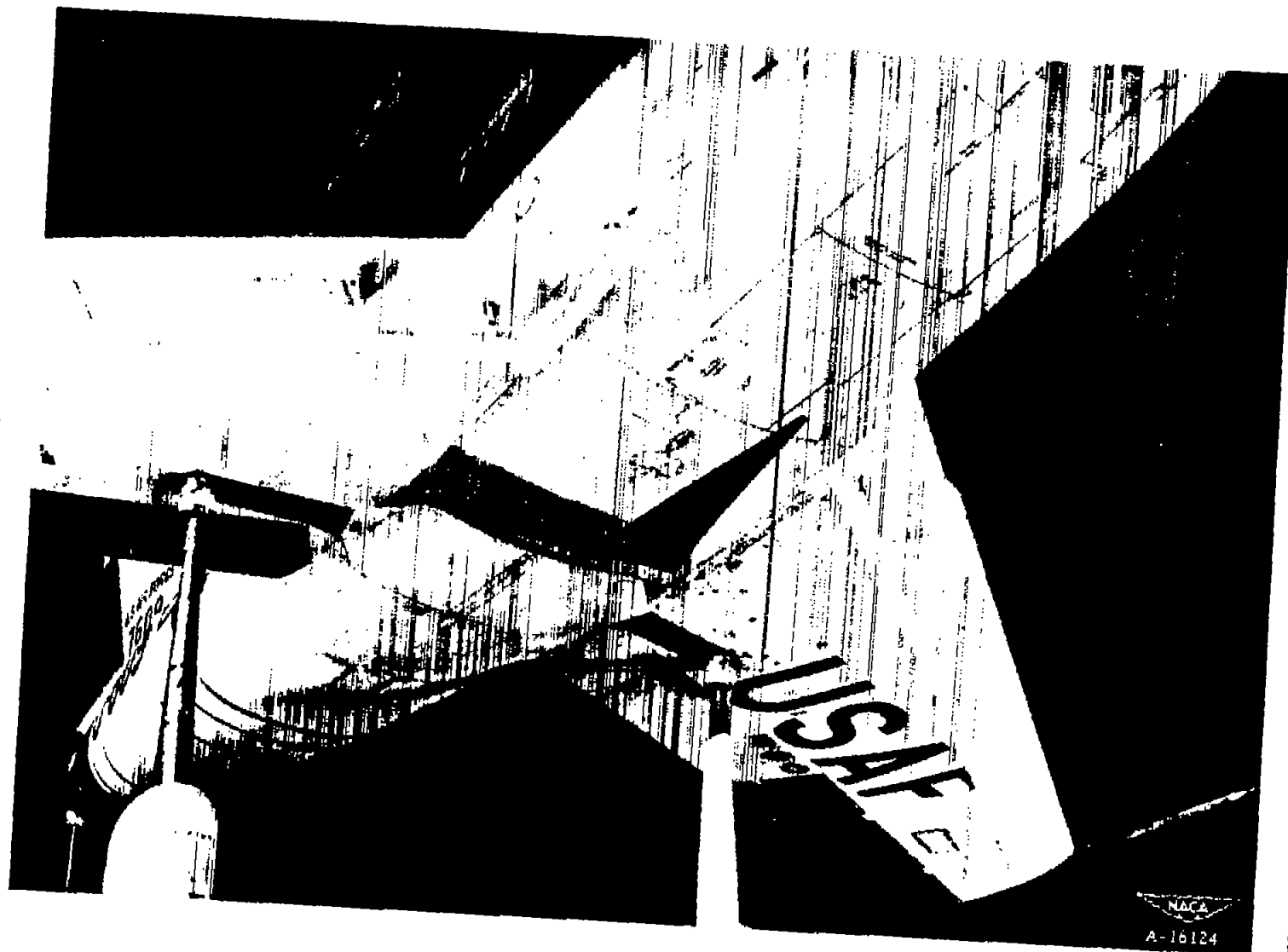
Detail B — Wing mod. 3



Section x-x enlarged



Figure 5.— Details of wing modifications 2 and 3.



NACA RM A52B05

Figure 6.— View of wing modification 2 on test airplane.



Figure 7.- View of wing modification 3 on the test airplane.



Figure 8.- View of the horizontal tail installed in the lower position.

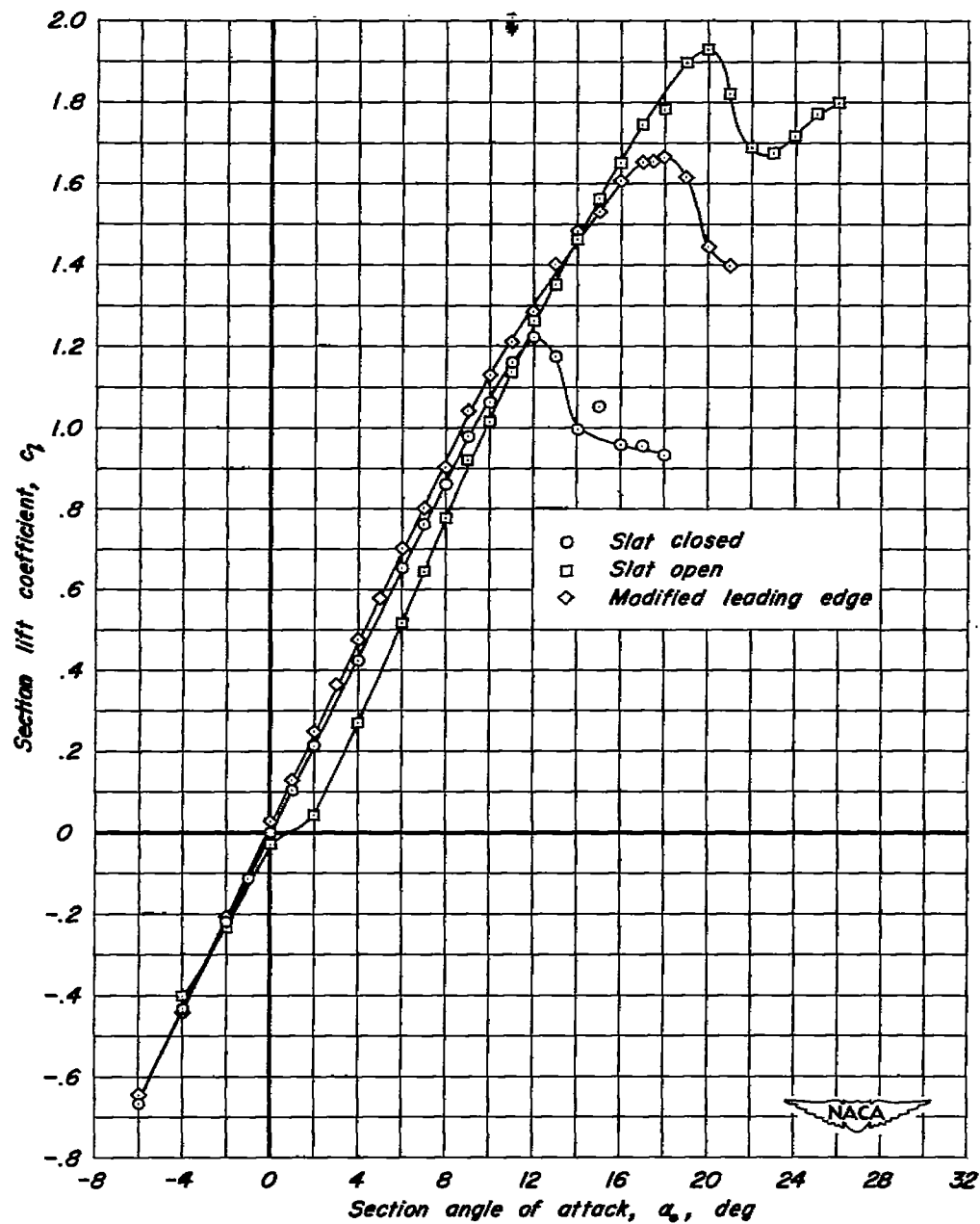
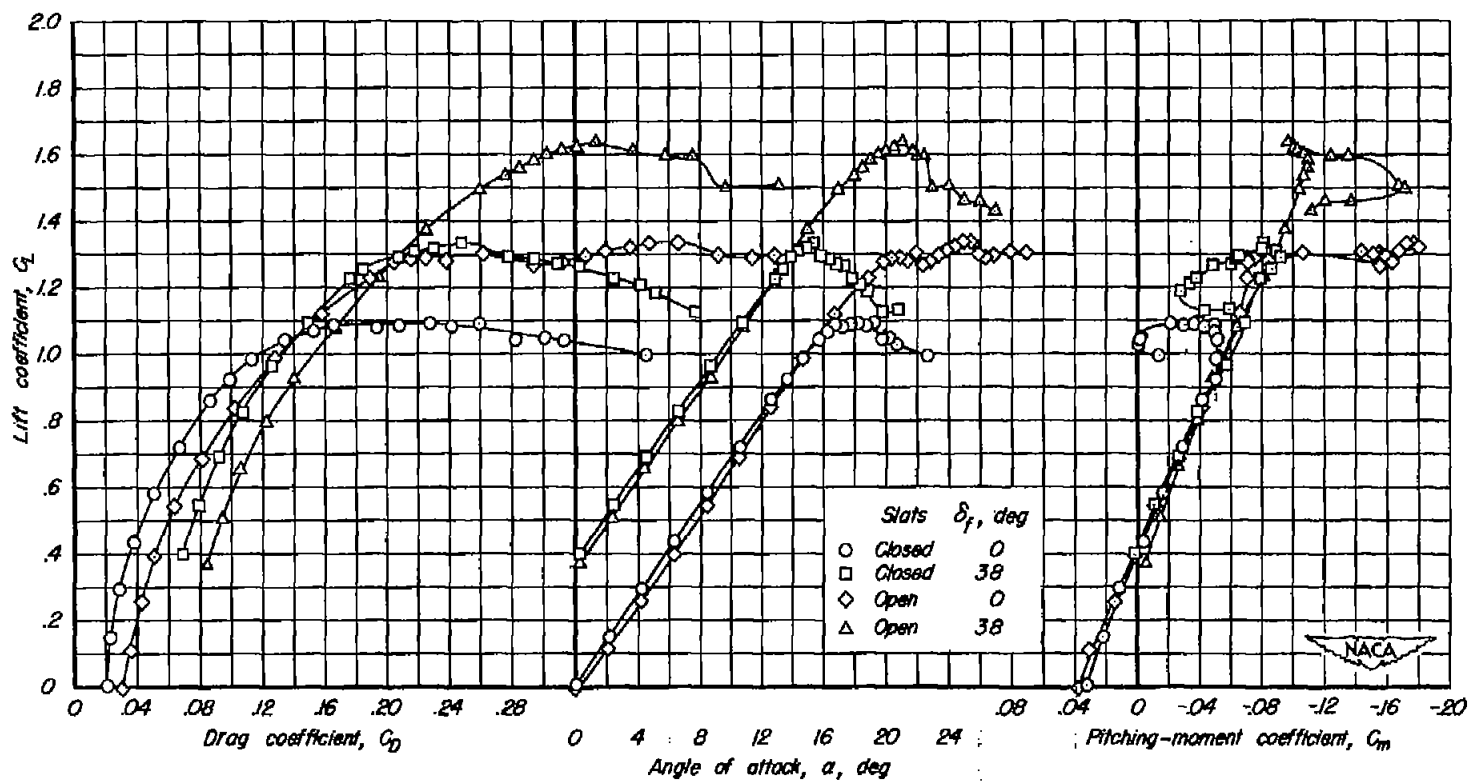


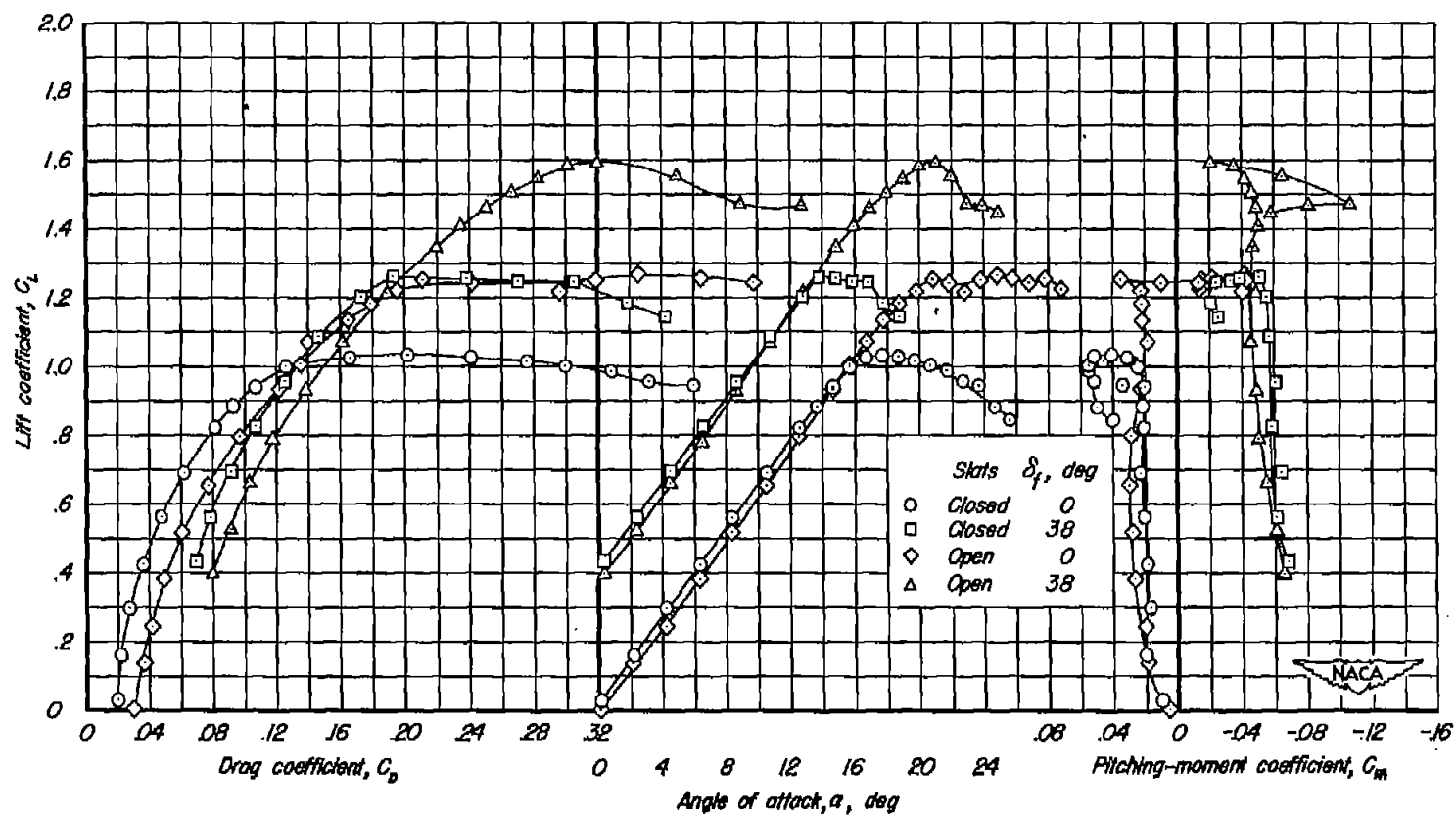
Figure 9.—Two-dimensional lift curves for the wing section normal to the wing quarter-chord line at 0.857 semispan with slat closed and open and with the modified leading edge. $R, 2.1 \times 10^6$.



(a) Horizontal tail in the normal position.

M = 0.16

Figure 10.- Aerodynamic characteristics of the test airplane with the unmodified wing. $R, 8.4 \times 10^6$.



(b) Horizontal tail off.

Figure 10.- Concluded.

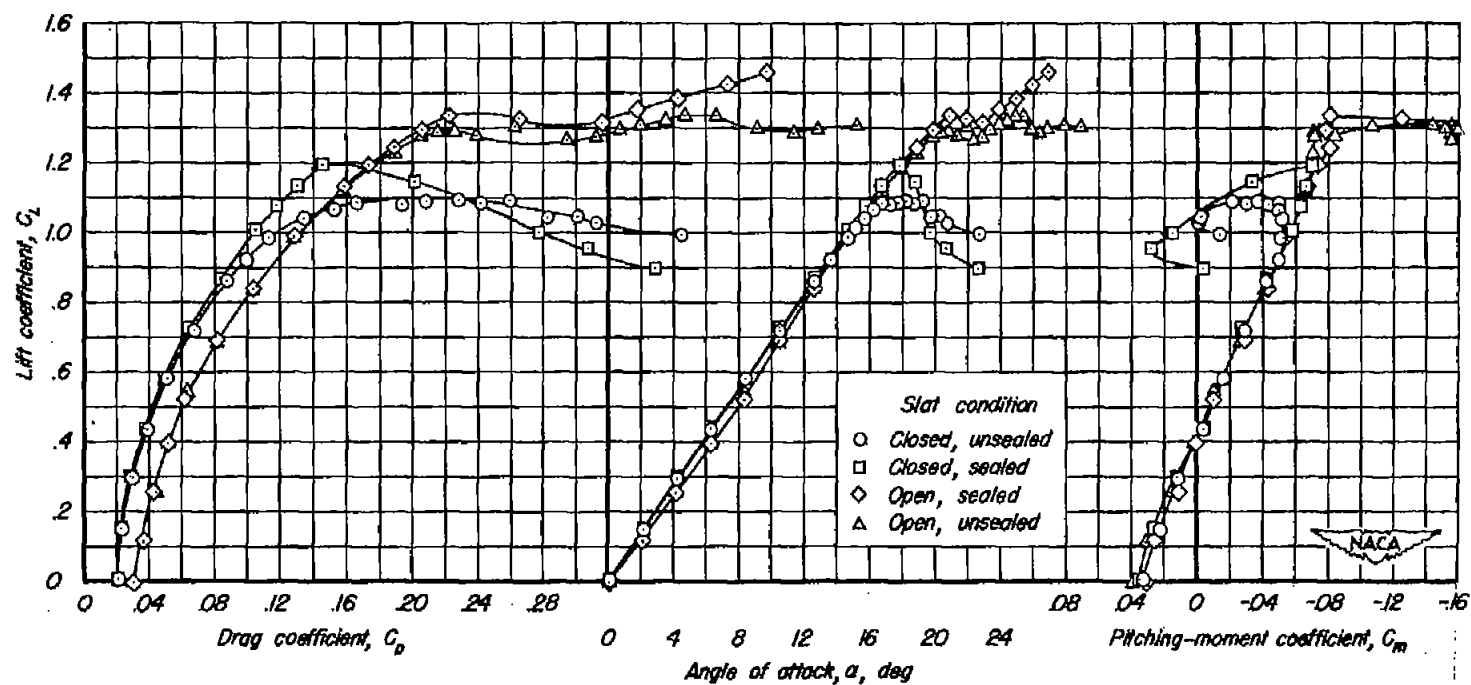
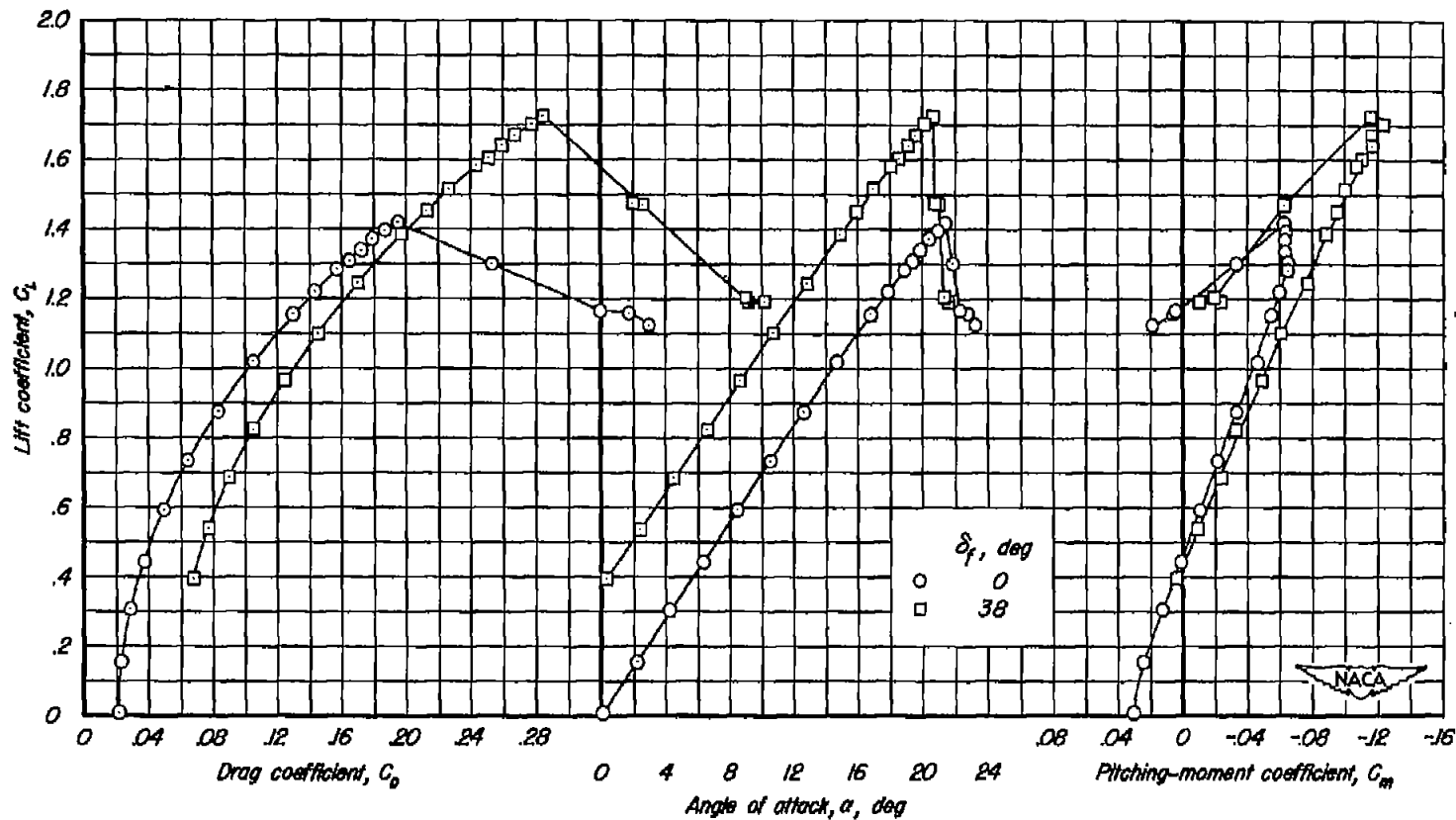
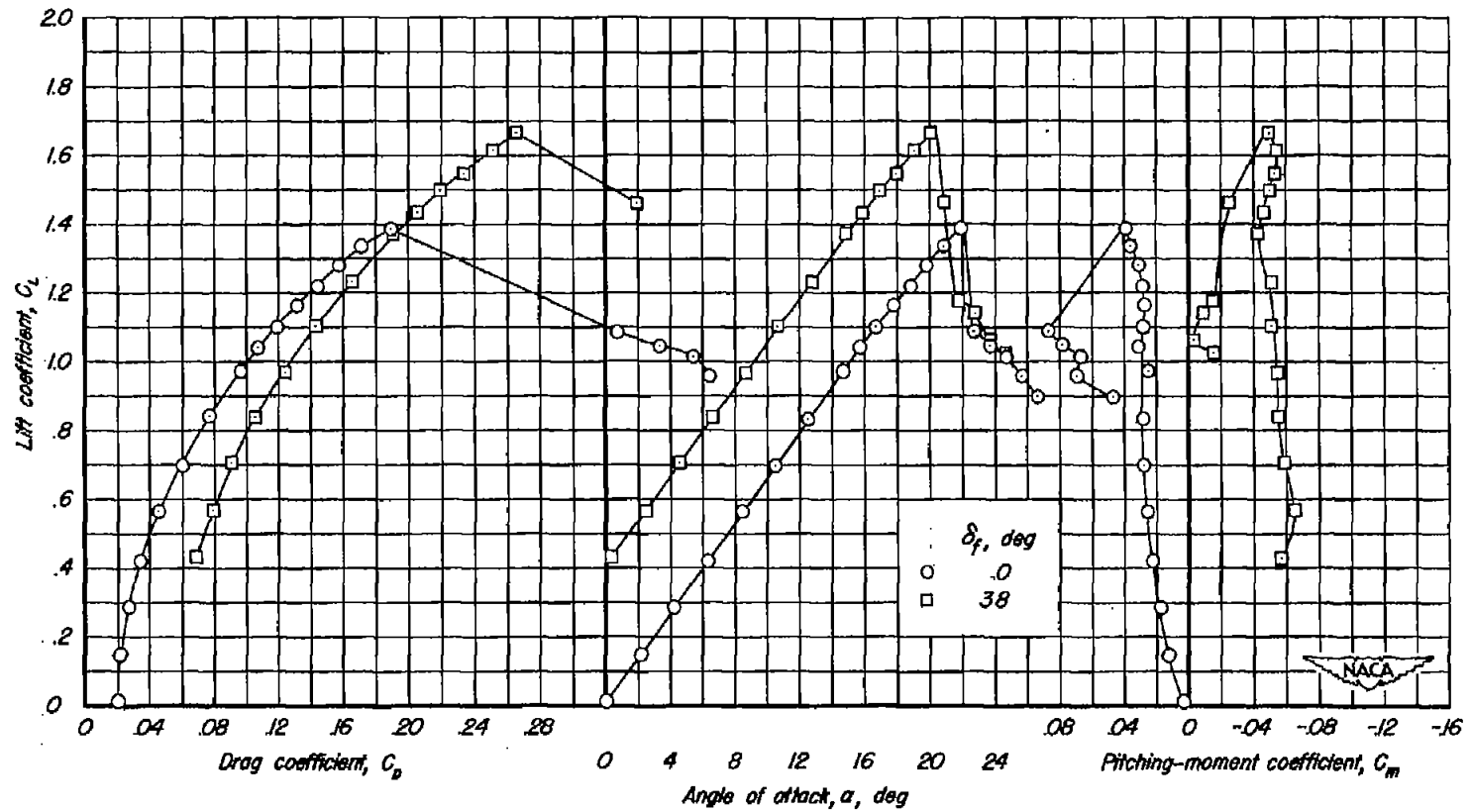


Figure 11.— Effects of sealing the slats on the aerodynamic characteristics of the test airplane. Horizontal tail in the normal position; $R, 8.4 \times 10^6$.



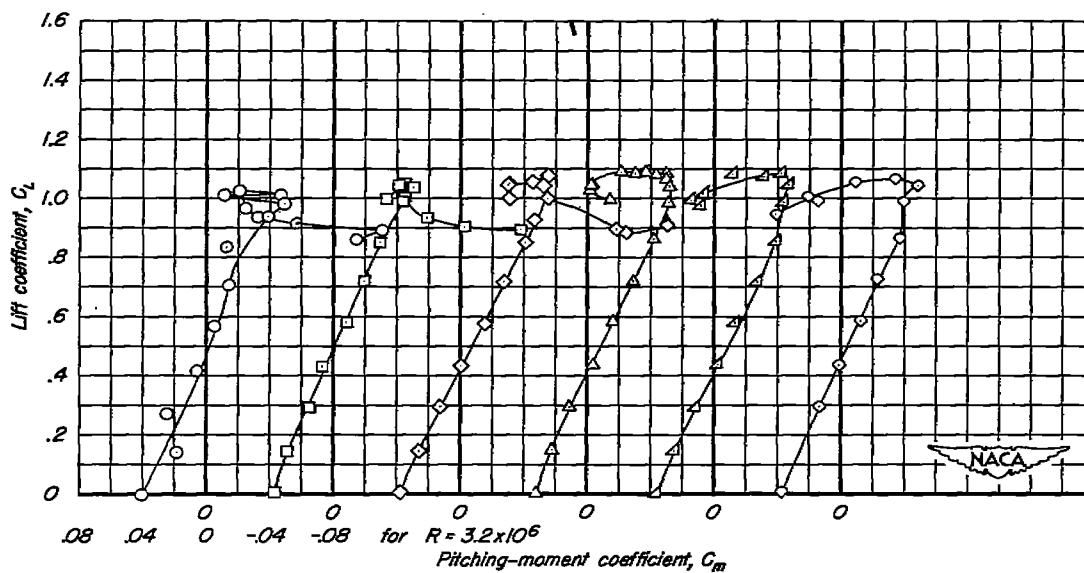
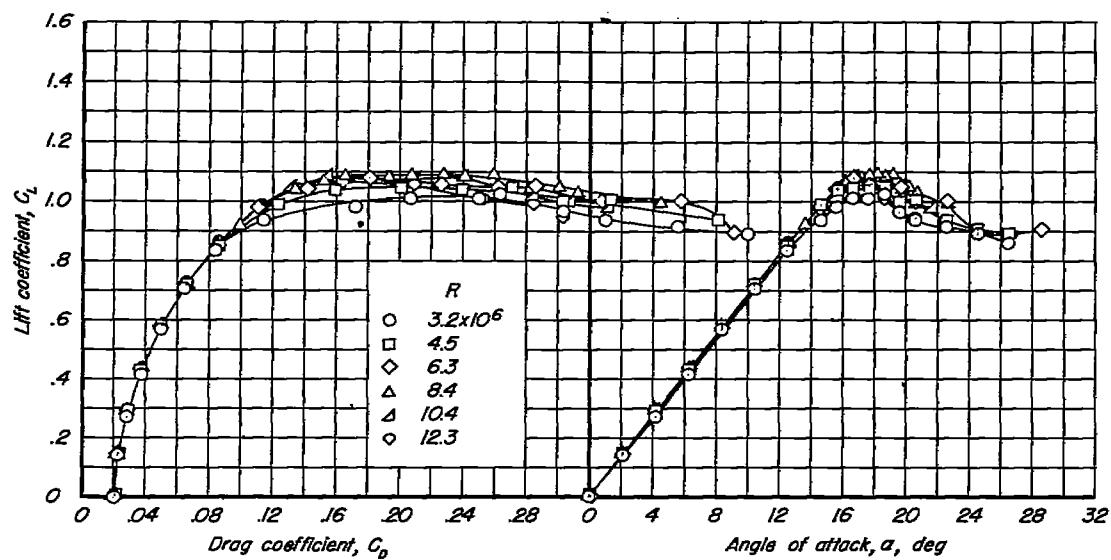
(a) Horizontal tail in the normal position.

Figure 12.- Aerodynamic characteristics of the test airplane with wing modification I. $R, 8.4 \times 10^6$.



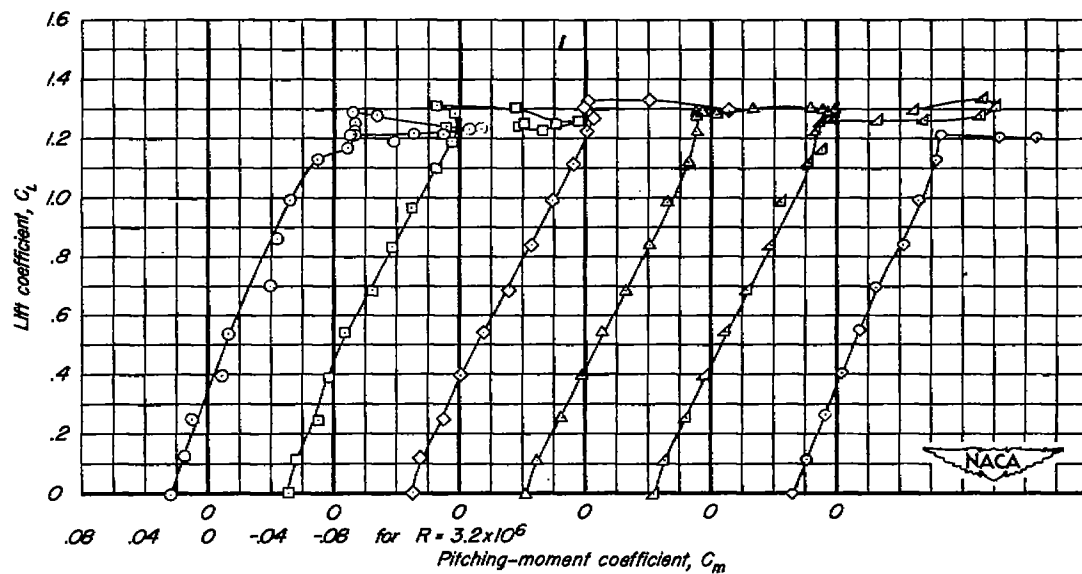
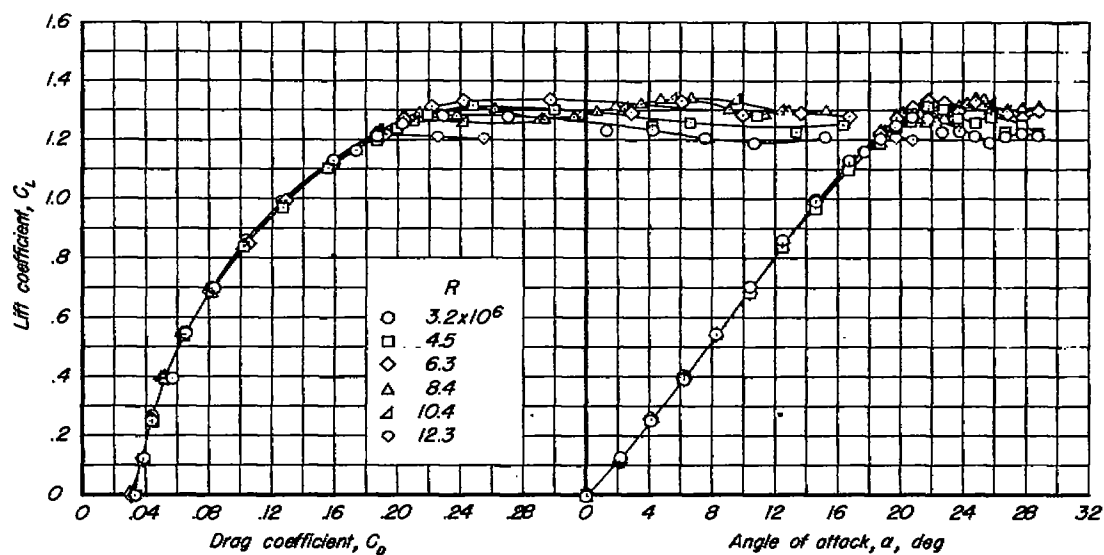
(b) Horizontal tail off.

Figure 12.- Concluded.



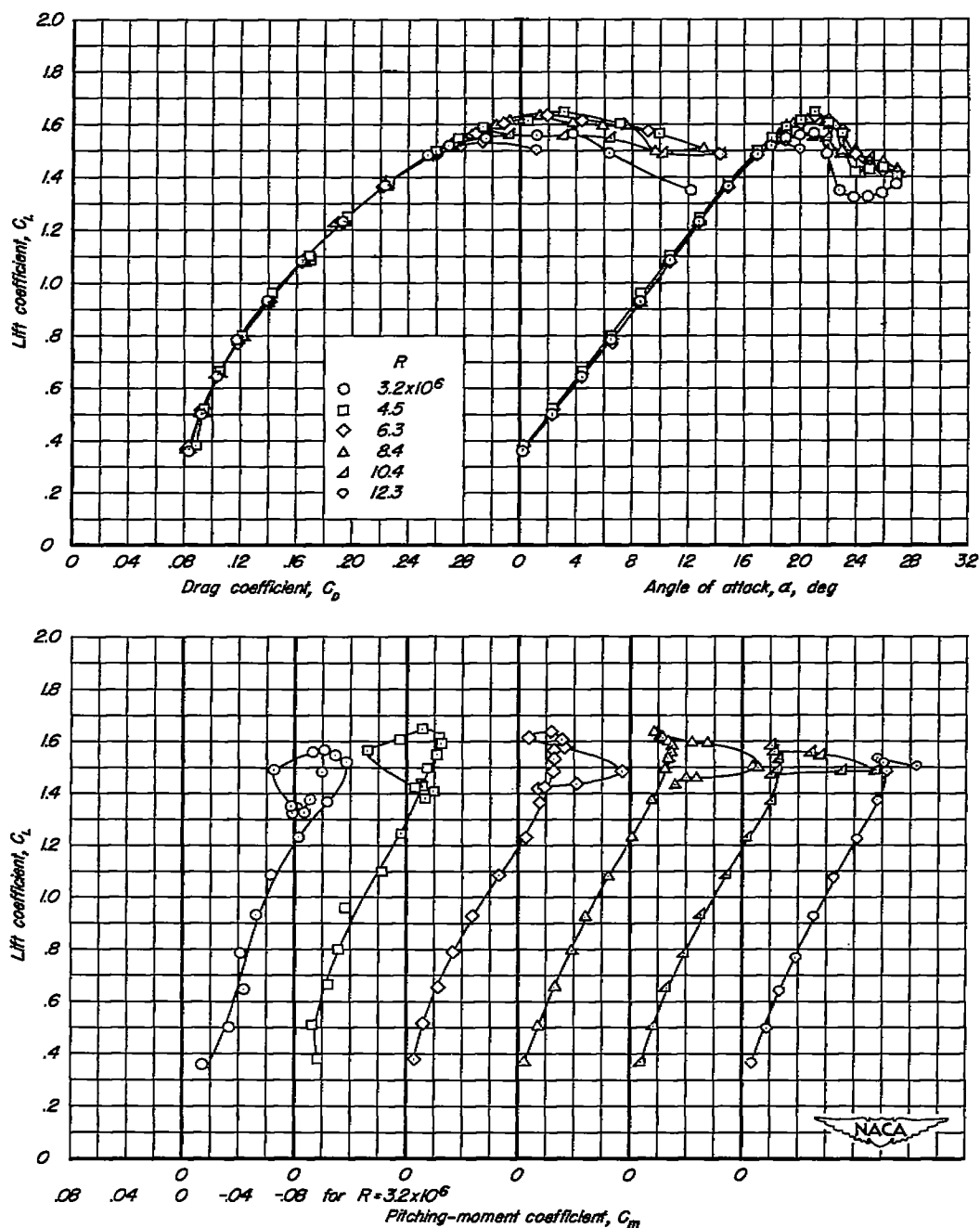
(a) Slats closed, flaps up.

Figure 13.- Reynolds number effects on the aerodynamic characteristics of the test airplane. Horizontal tail in the normal position.



(b) Slats open, flaps up.

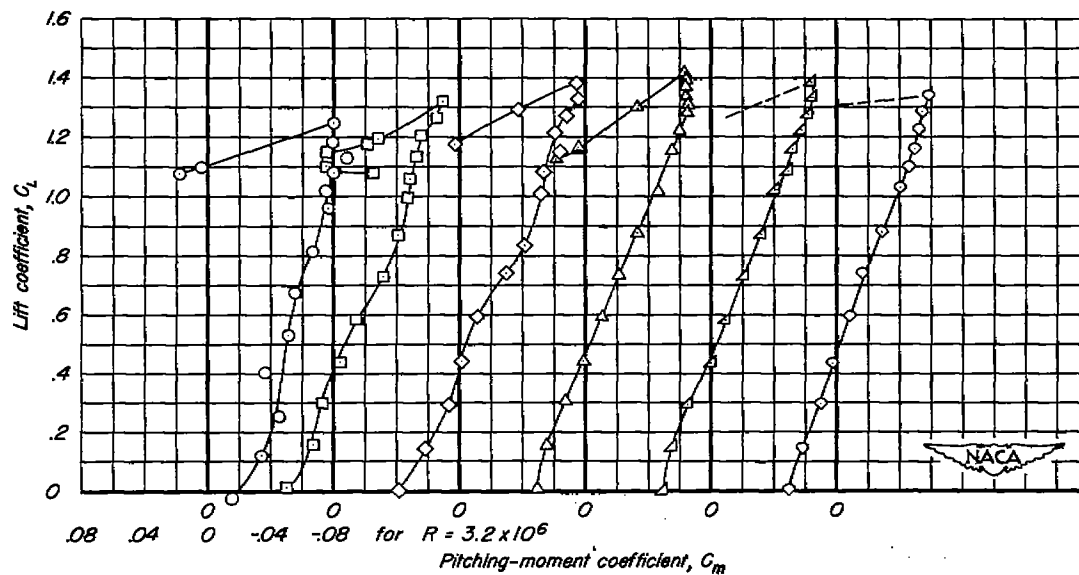
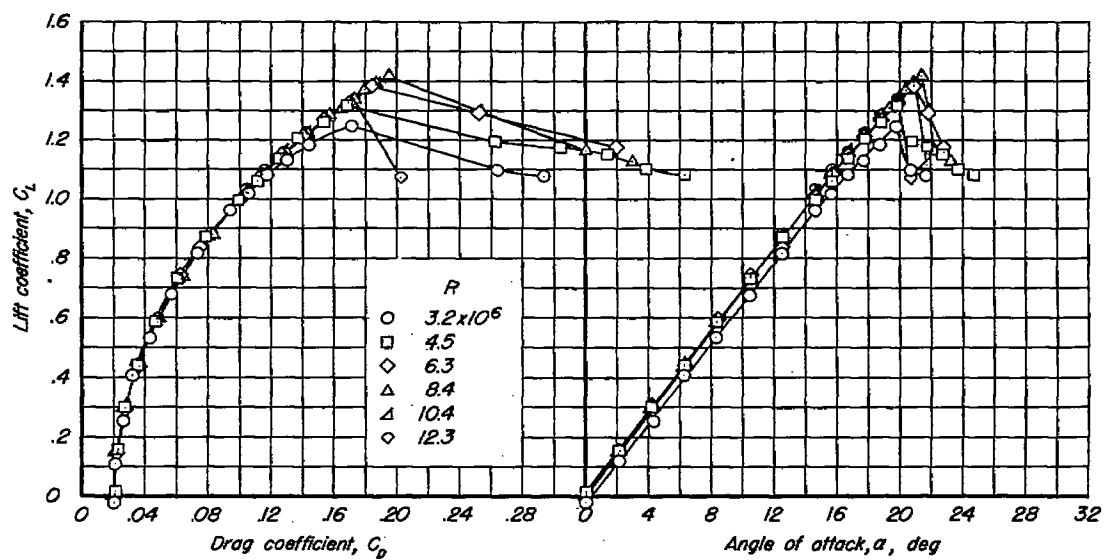
Figure 13.- Continued.



(c) Slats open, flaps down.

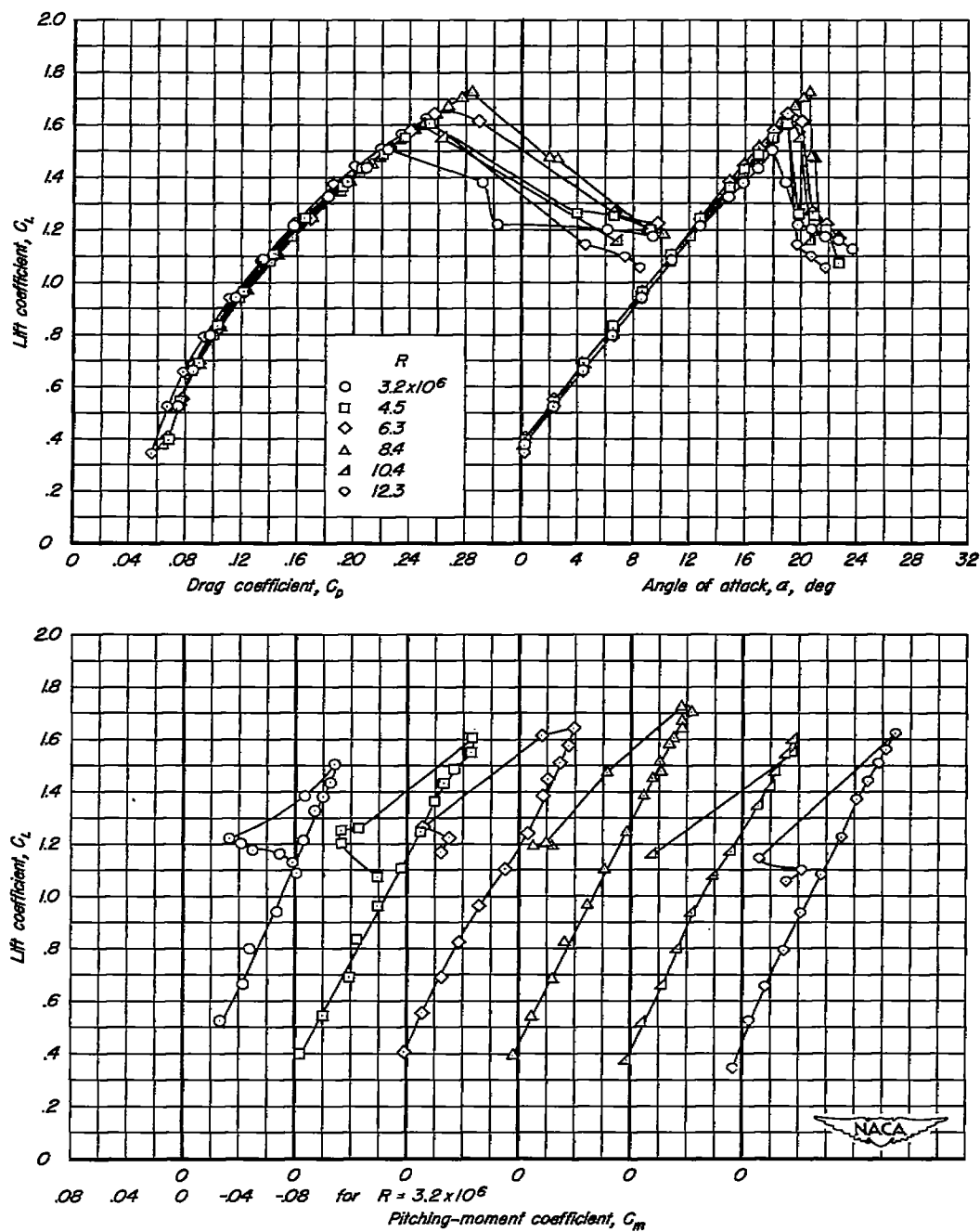
Figure 13.- Continued.

~~FIGURE 13.-~~



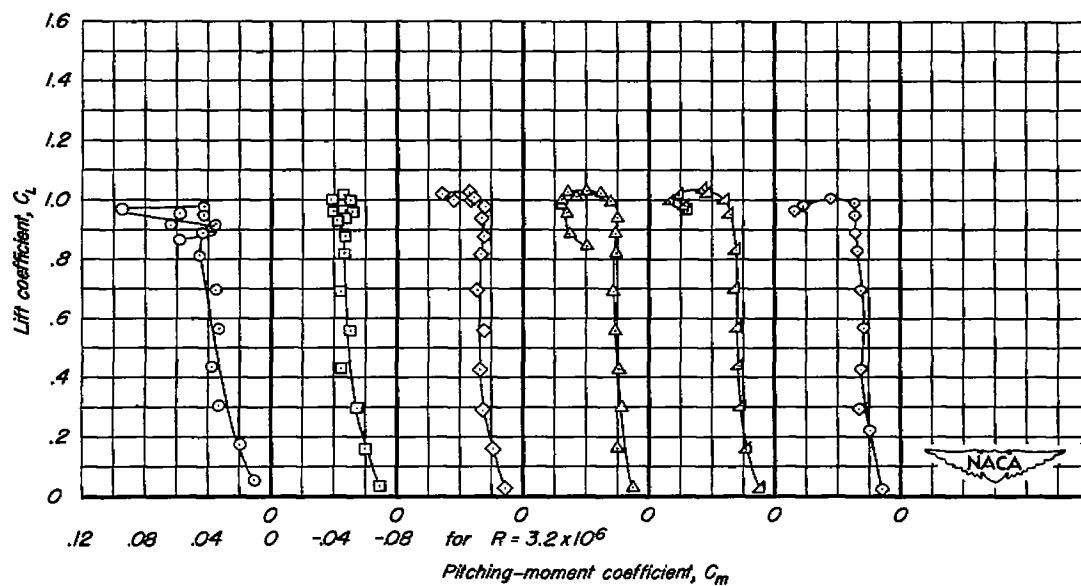
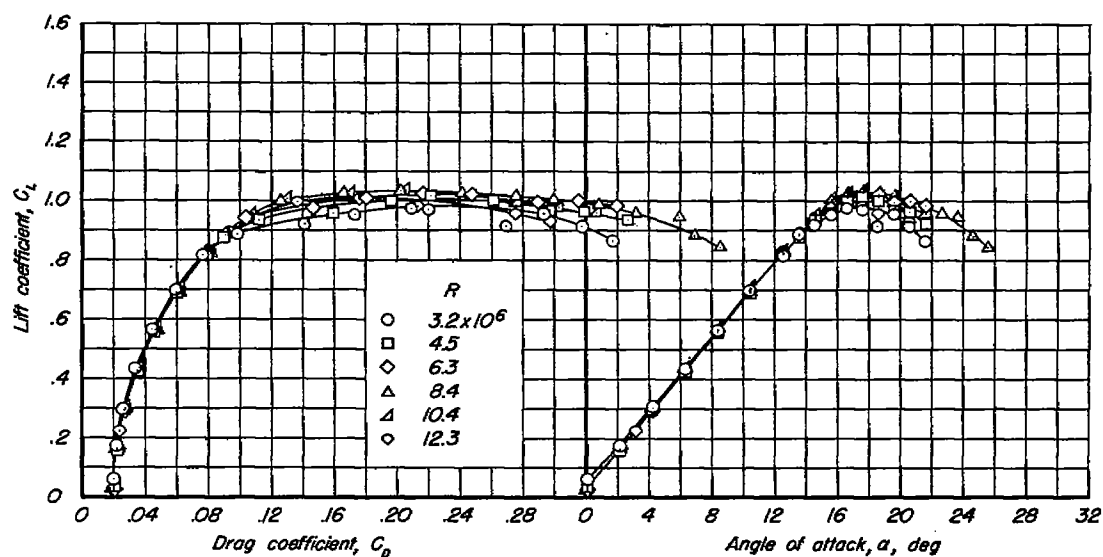
(d) Wing modification 1, flaps up.

Figure 13.- Continued.



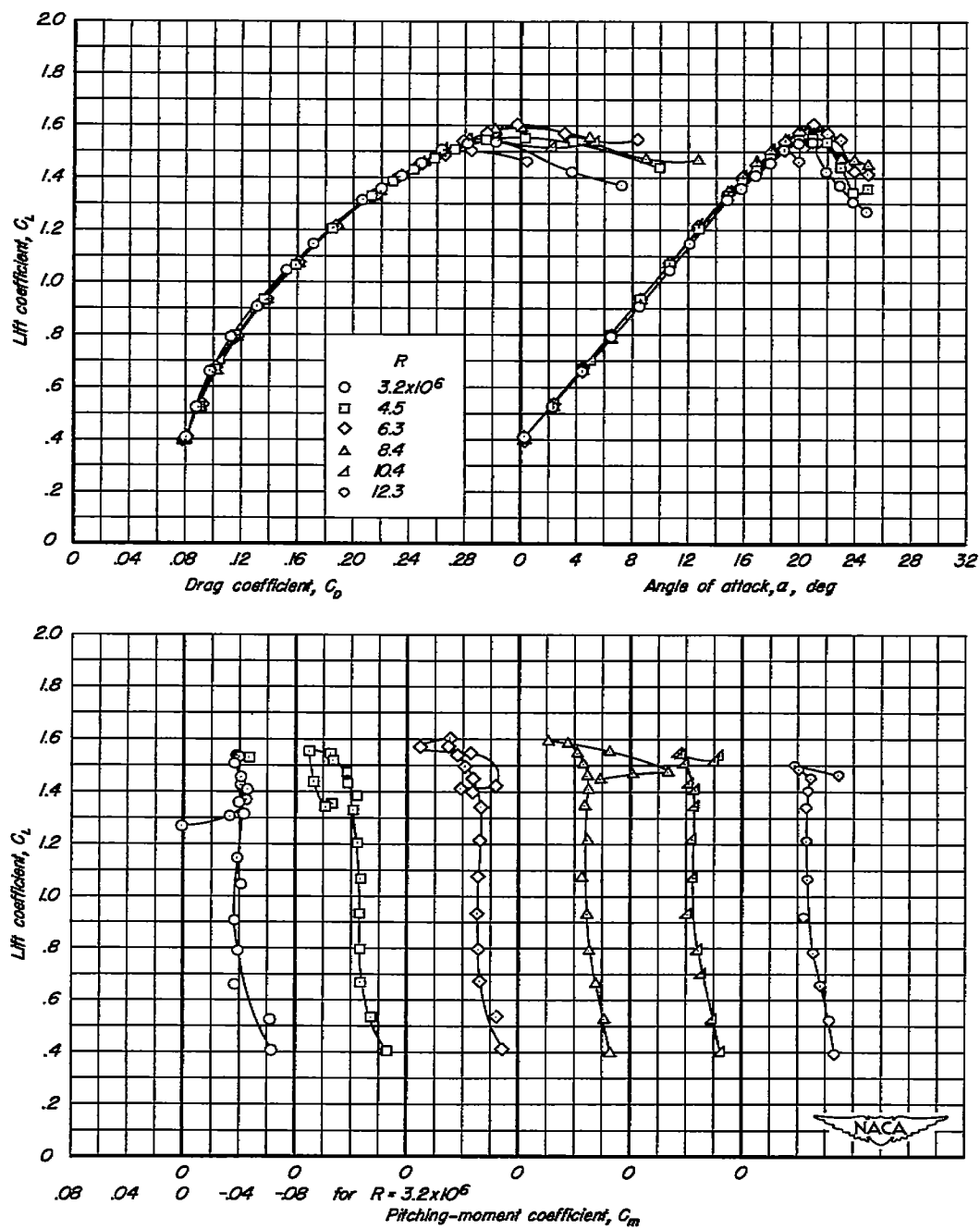
(e) Wing modification I, flaps down.

Figure 13.- Concluded.



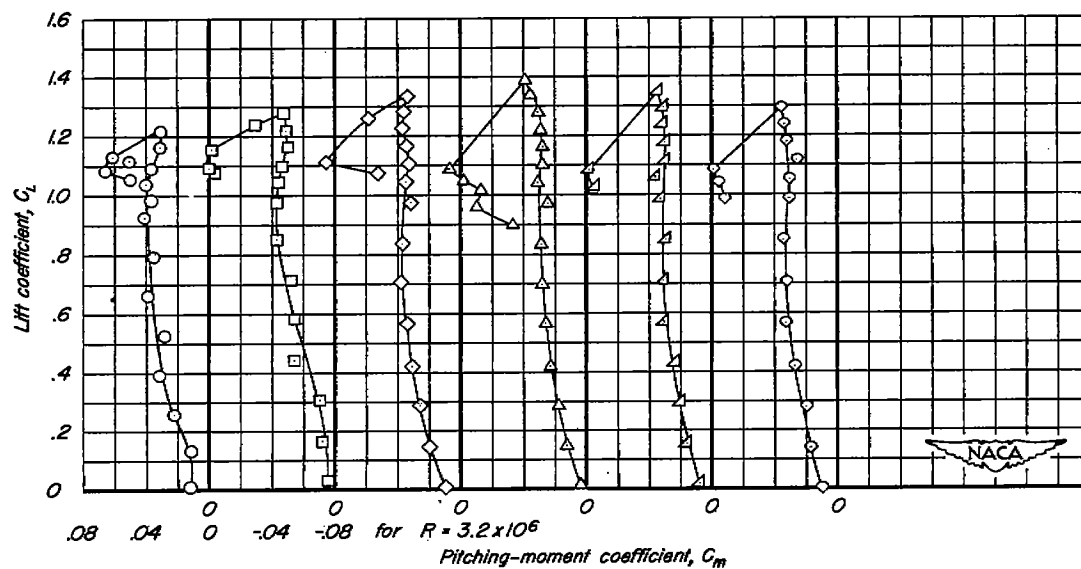
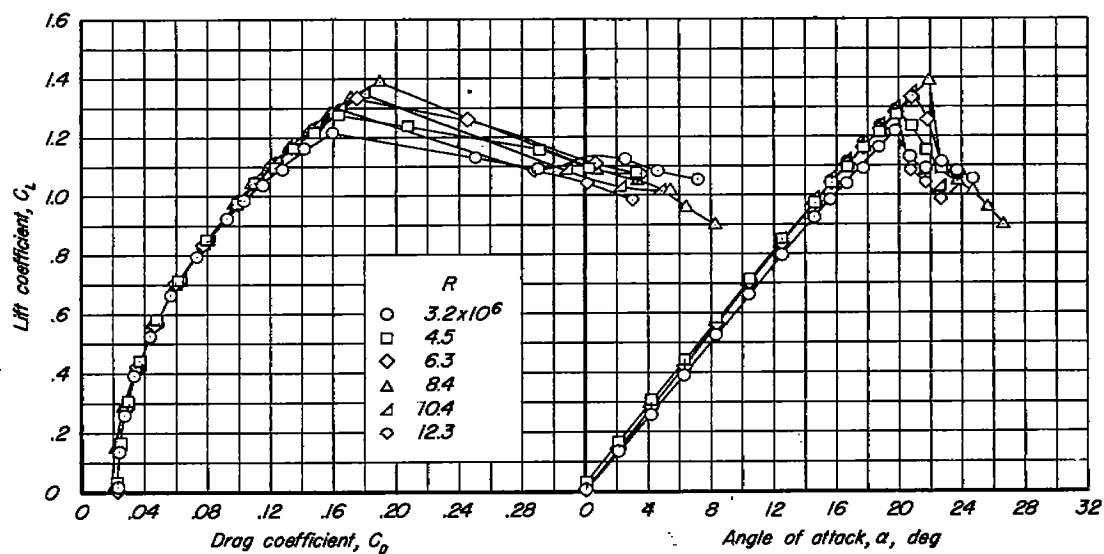
(a) Slats closed, flaps up.

Figure 14.- Reynolds number effects on the aerodynamic characteristics of the test airplane. Horizontal tail off.



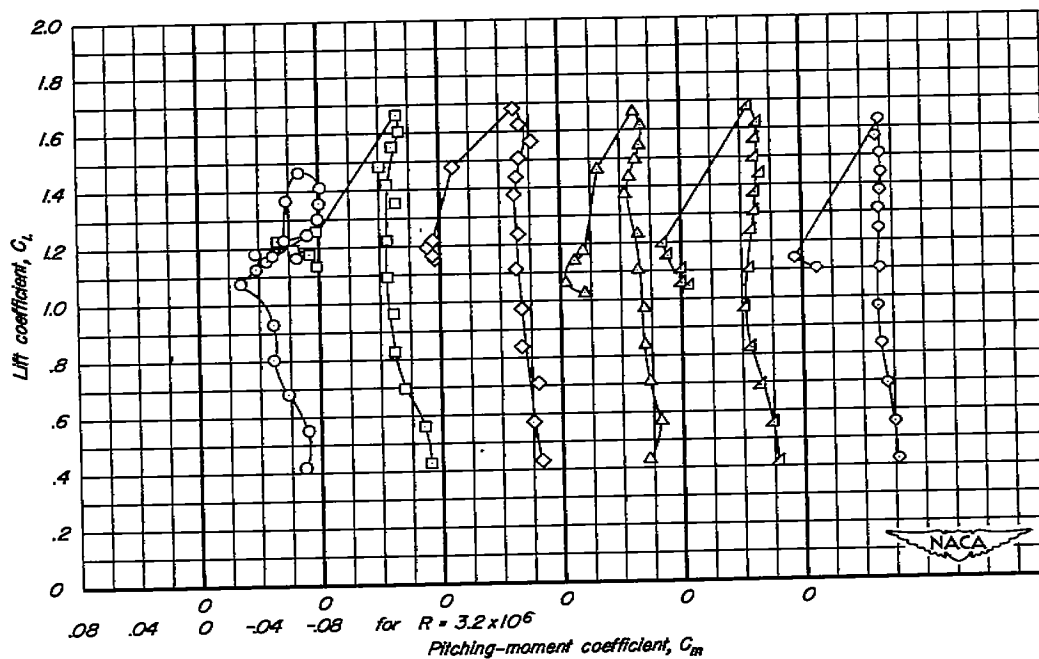
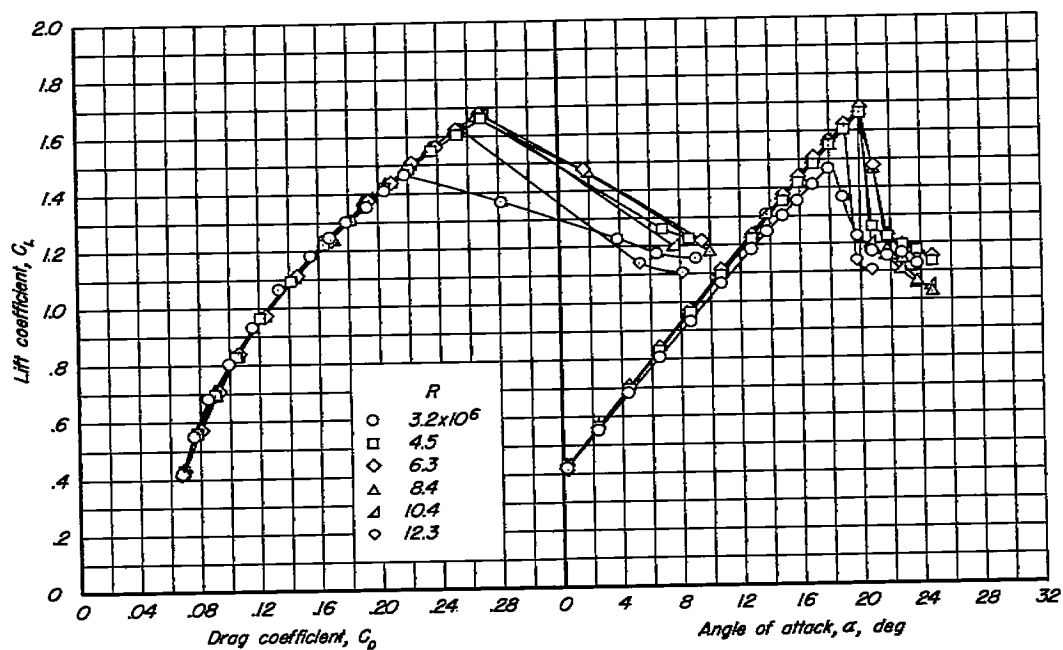
(b) Slats open, flaps down.

Figure 14.— Continued.



(c) Wing modification I, flaps up.

Figure 14.- Continued.



(d) Wing modification 1, flaps down.

Figure 14.- Concluded.

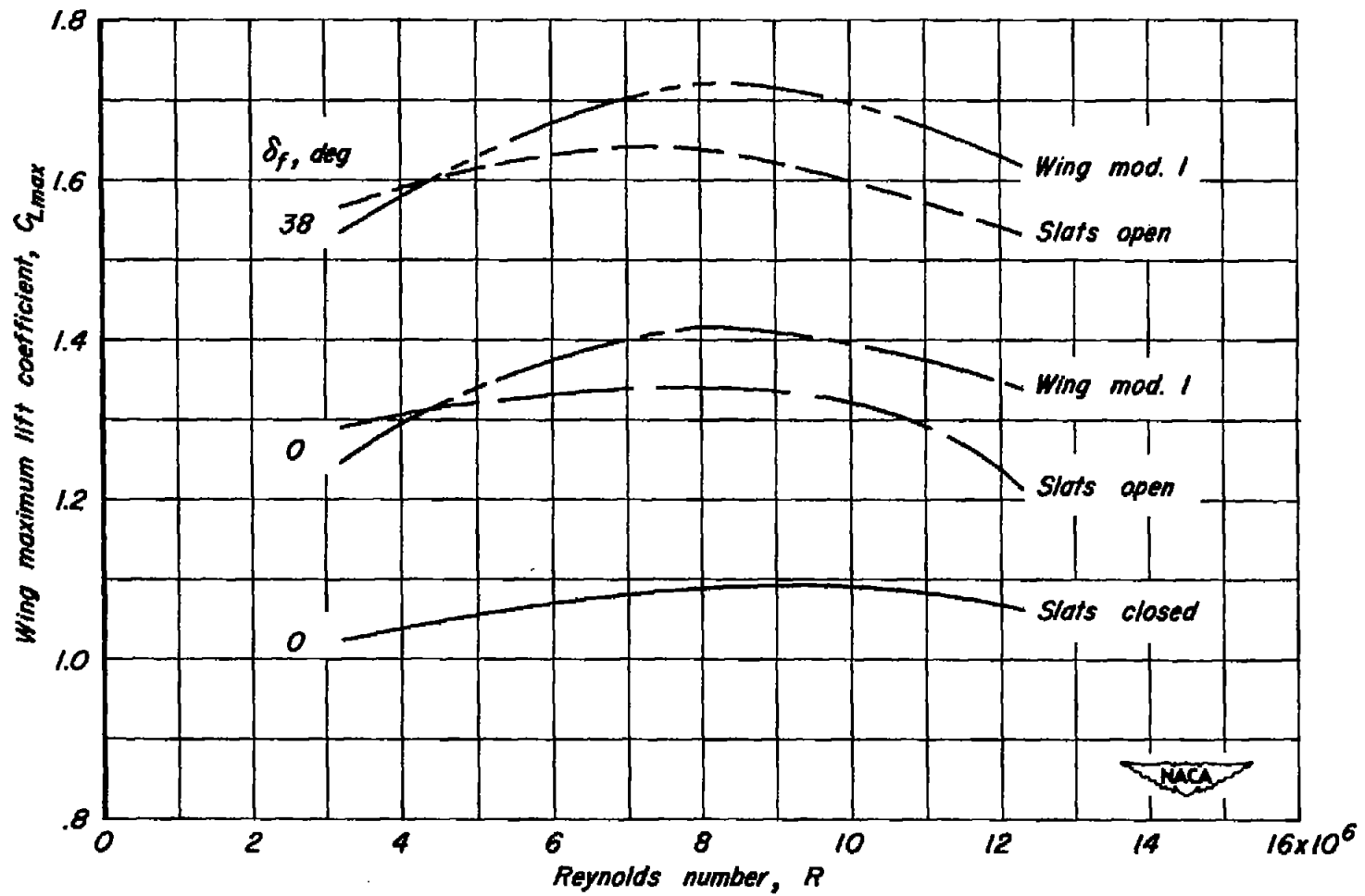
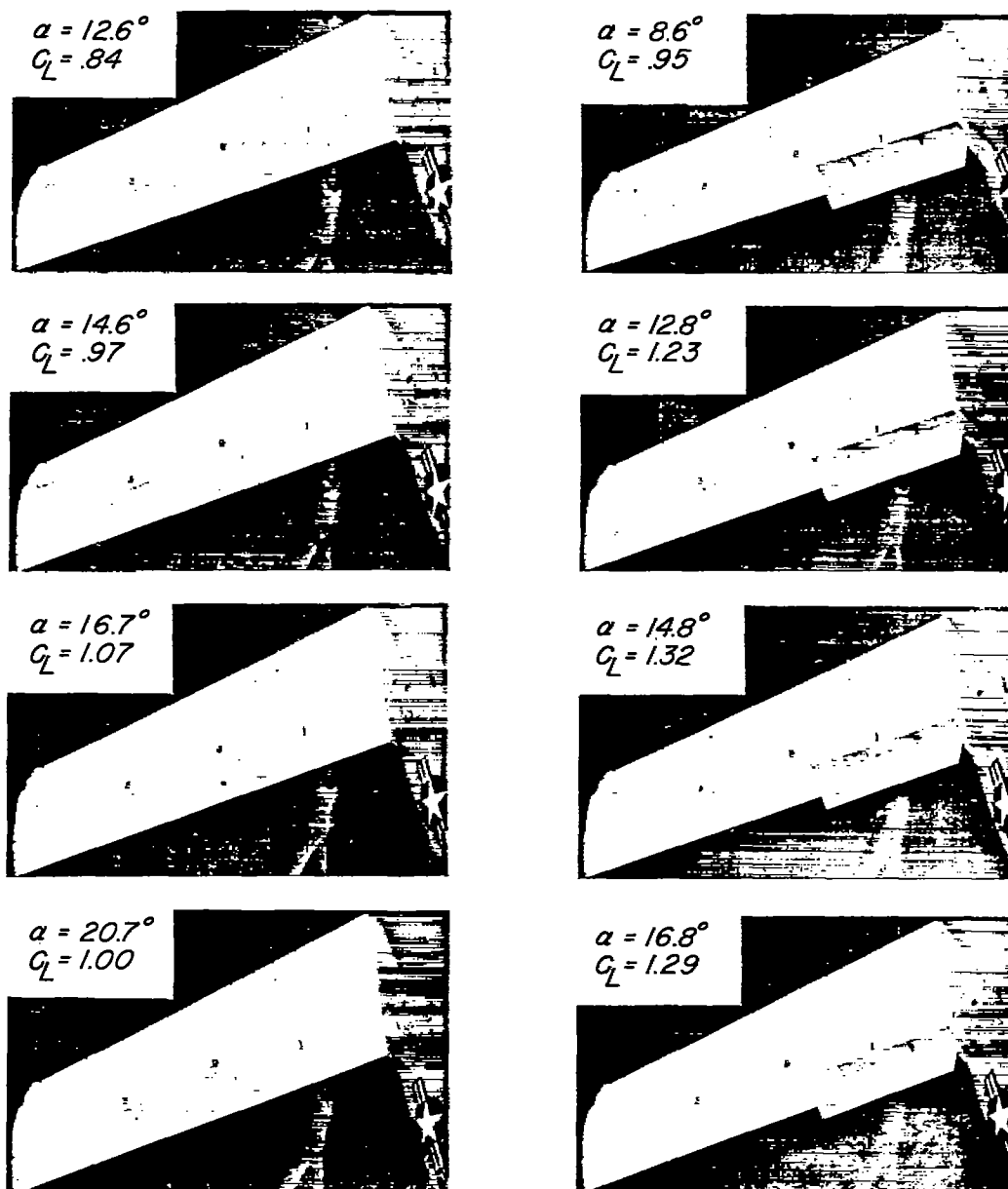
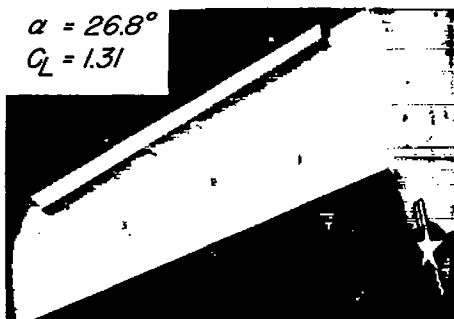
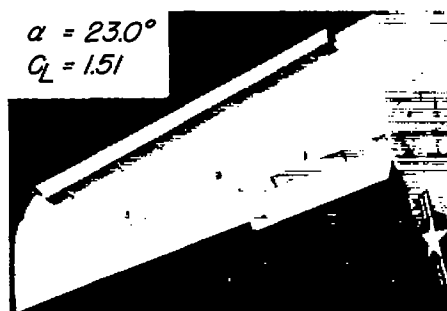
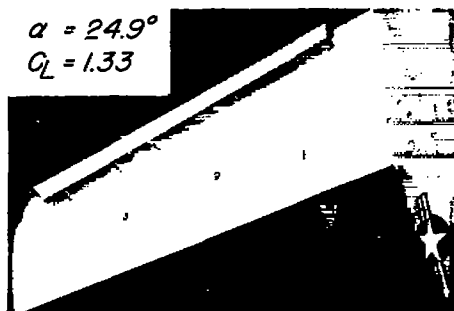
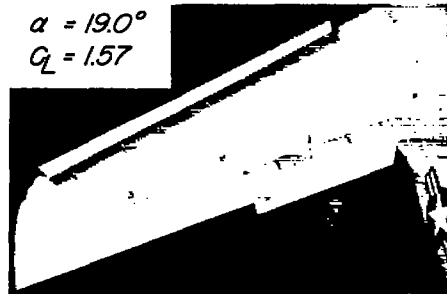
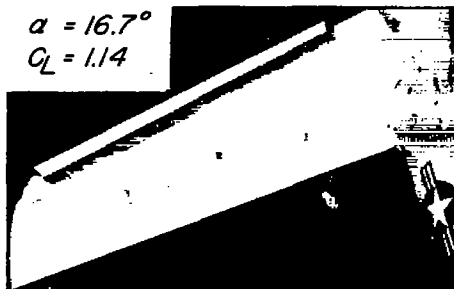


Figure 15.— Reynolds number effects on maximum lift. Horizontal tail in the normal position.

(a) Slats closed, $\delta_f = 0^\circ$.(b) Slats closed, $\delta_f = 38^\circ$.

NACA
A-16750

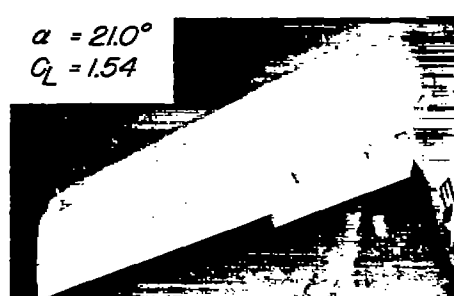
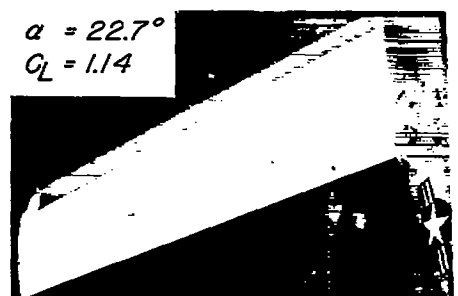
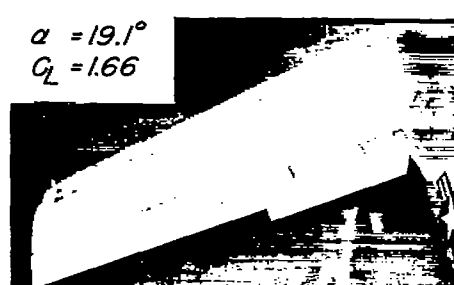
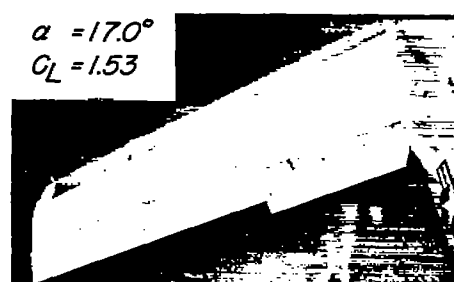
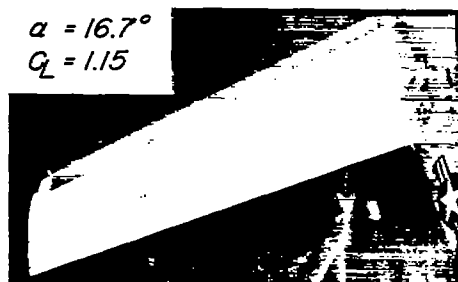
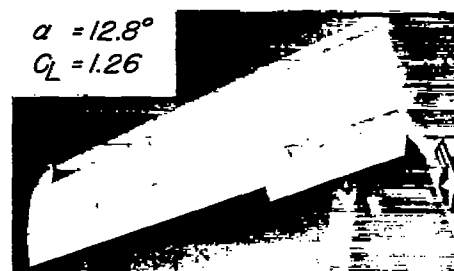
Figure 16.- Studies of tuft action on the left wing for several wing configurations. Horizontal tail in the normal position; $R, 8.4 \times 10^6$.



(c) Slats open, $\delta_f = 0^\circ$.

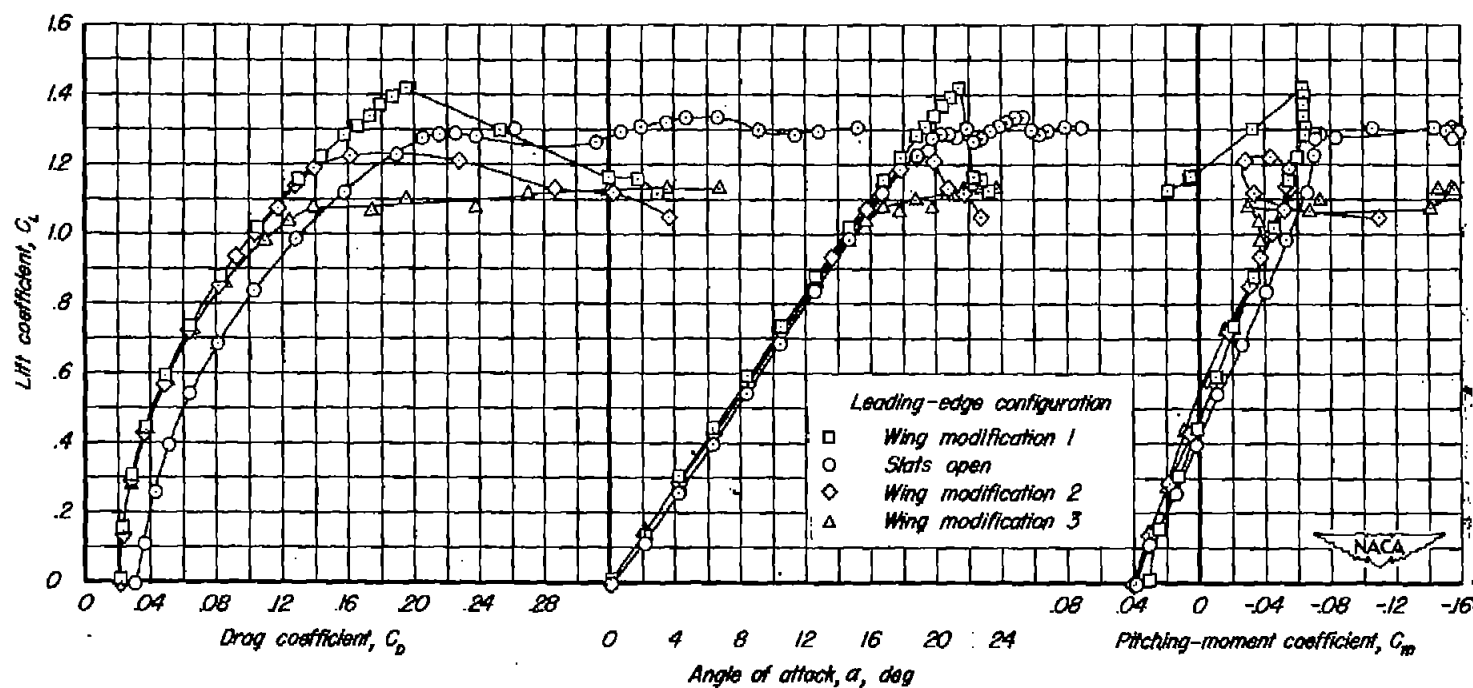
(d) Slats open, $\delta_f = 38^\circ$.

Figure 16.— Continued.



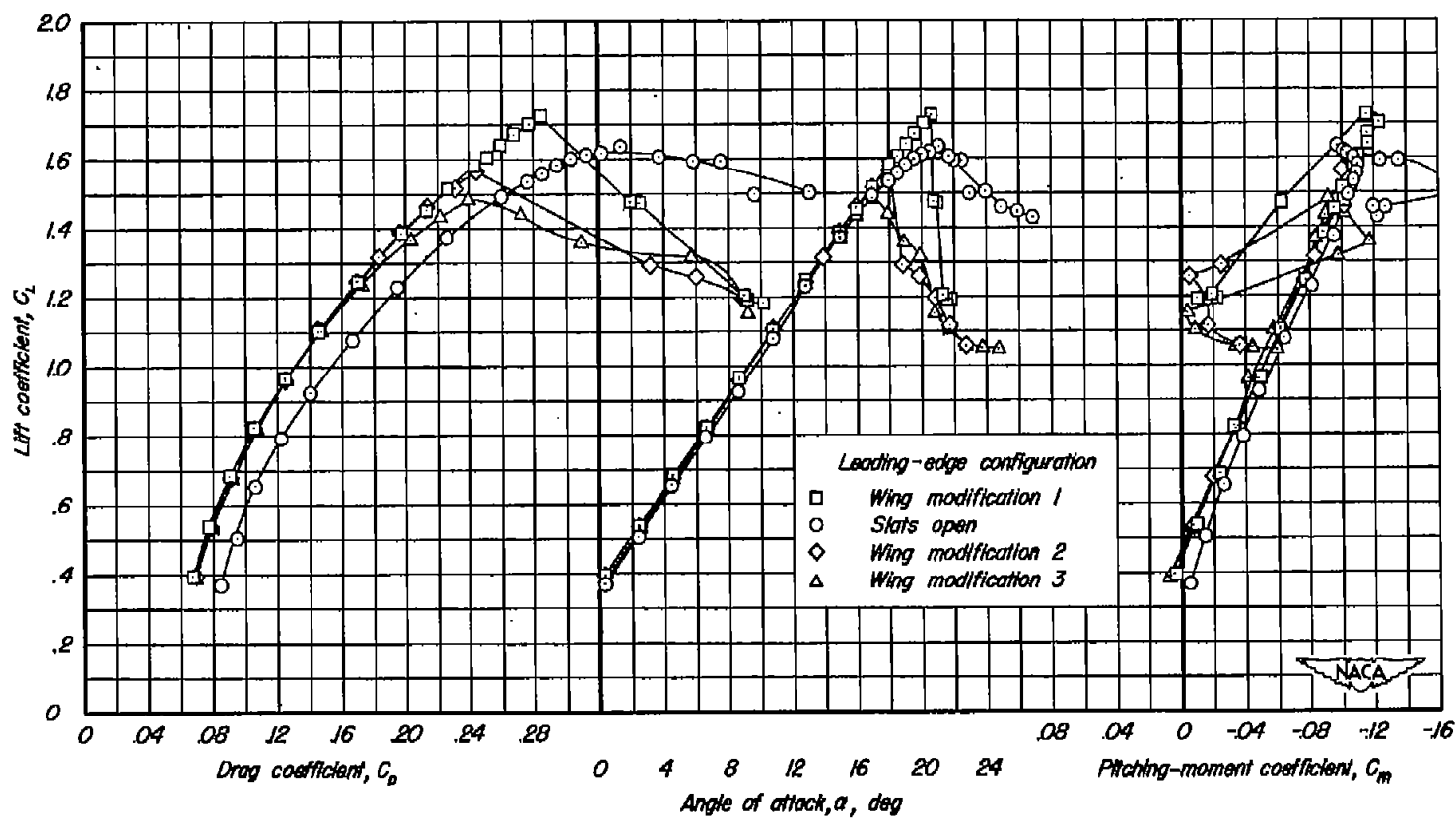
(e) Wing mod. I, $\delta_f = 0^\circ$.

(f) Wing mod. I, $\delta_f = 38^\circ$.



(a) Flaps up.

Figure 17.— Comparisons of the effects of wing modifications 1, 2, and 3 with the effects of the slats on the aerodynamic characteristics of the test airplane. Horizontal tail in the normal position; $R, 8.4 \times 10^6$.



(b) Flaps down.

Figure 17.- Concluded.

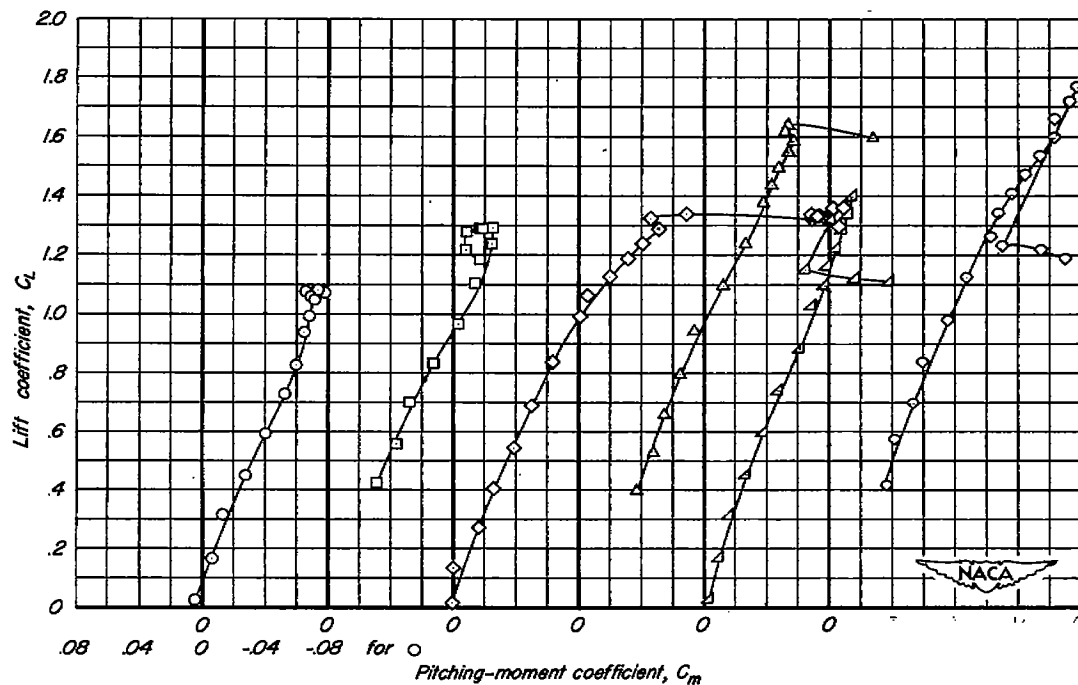
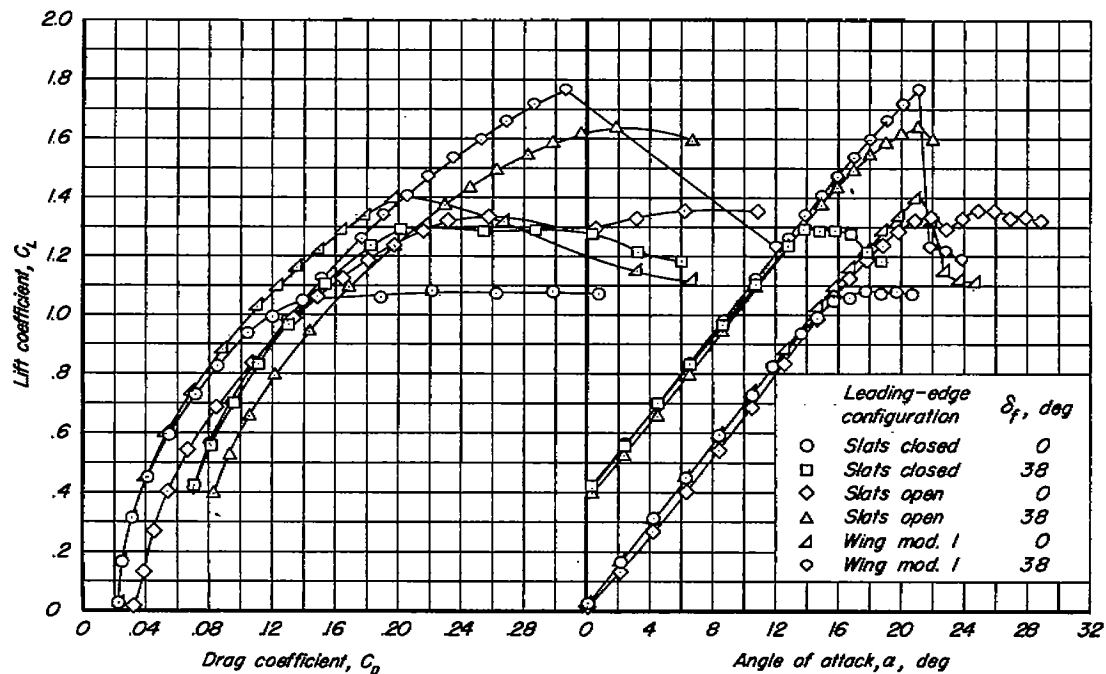


Figure 18.—Aerodynamic characteristics of the test airplane with the horizontal tail at a lower position. $R, 8.4 \times 10^6$.

SECURITY INFORMATION



[REDACTED]

[REDACTED]